ARKIV FÖR ASTRONOMI Band 5 nr 20

Read 9 April 1969

A study of physical groups of galaxies

By Erik Holmberg

CONTENTS

ABSTRACT

This paper presents the results of an investigation of 174 physical groups of galaxies, most of them presumably comparable to the Milky Way and M31 groups (= Local Group), and the M81 group. The groups selected are centered on prominent spiral galaxies, for which the distance moduli can be estimated. The survey work has been based on the Palomar Sky Atlas, the prints being evaluated down to the practical limit, as regards galaxies; the limiting diameter of the group members is 0.6 kpc, and the limiting absolute pg magnitude about −10.6. On account of the large disturbances from the background–foreground fields it has been necessary to restrict the survey to

circular areas with a radius of 50 kpc around the central spiral galaxies. Areas of this size probably include about 30 % of all the satellites. A summary of the observational data is given in Table 7.

In the case of spiral galaxies with an edgewise orientation, the physical satellites have a peculiar distribution; most of them are found along the elongation of the minor axis, and they thus seem to favor high local latitudes (sect. 7). The number of satellites seems to be larger for spirals with exceptionally blue nuclei (such nuclei often appear to be abnormal) and for spirals with large hydrogen masses (sect. 8–9). The results favor the hypothesis that the satellites are produced by matter ejected from the nuclear regions of the spiral systems. The statistical evidence is however not conclusive.

The distribution of the log. abs. diameters of all the members of the physical groups can be transformed into a distribution of abs. magnitudes by means of the correlation diagram of Fig. 9. Luminosity functions have been determined for the E–So–Ir and Sa–Sb–Sc groups separately. The curves of Figs. 8 and 10 are based on a total of about 370 galaxies, and extend from $M = -10.6$ to $M = -22$. The log. distribution referring to the E–So–Ir group is a straight line with an inclination of 0.2; the Sa–Sb–Sc spirals can be represented by a normal error-curve, extending from $M = -15$ to $M = -22$. The results are supported by luminosity curves derived from redshifts.

The smothed-out space density of galaxies (outside the big clusters) has been determined from magnitudes, diameters, and redshifts; the result is 0.17 per Mpc^3 ($M < -15.0$). Reasonable assumptions, as regards the mass/lum. ratios for different types of galaxies, lead to a mass density of $2.5 \cdot 10^{-31}$ $\mathrm{gr/cm}^3$. The statistical distribution of the log. masses, referring to the members of the physical groups, is reproduced in Fig. 12. The distribution covers an interval of log. mass (solar units) from 8 to 12.

Chapter I. Introduction

1. Groups of galaxies

It seems to be a recognized fact that a considerable number of the galaxies in the general field (in this paper the term "general field" will be used to designate the space outside the big clusters) are not isolated objects but rather members of groups. Even a superficial examination reveals that some of the nearby giant spiral systems are surrounded by clouds of smaller and larger satellites. A detailed study of such physical groups would be of great importance, since it could furnish valuable information about a galaxian population in a given volume of space, especially as regards the statistical distributions of absolute characteristics, such as luminosities, diameters, and masses. If the group members form a representative sample of all general field galaxies, the results would be of universal significance. It may not be necessary to point out that information of this type is very hard, if not impossible, to obtain for low-luminosity galaxies by other methods, on account of the difficulty in determining individual distances. In the case of a physical group the central dominant galaxy serves as a distance indicator.

In a previous investigation the writer (1950) has presented some results referring to groups of galaxies. The distribution curves derived for absolute luminosities and diameters were of a very preliminary nature, since they referred only to members of the Local Group, the M81 group, and the M101 group.

The present paper gives the results of a study of physical companions belonging to 174, more or less nearby, prominent spiral galaxies. The investigation is based on plates previously taken with the Mount Wilson 60-inch and 100-inch telescopes (cf. Holmberg 1958, 1964), and on the prints of the National Geographic Society–Palomar Observatory Sky Atlas, the latter being evaluated down to the practical limit, as regards gal-

axies. From an examination of over 3000 galaxies in circular survey areas around the spiral systems and in nearby comparison areas, a total of 274 physical companions has been picked out. A summary of the material is presented in Tables 2 and 7. As will be shown in the following sections, the analysis leads to a series of interesting results, for instance, concerning the number of satellites, as related to different properties of the central spiral system, and as regards the luminosity functions of different types of galaxies.

As regards the important question whether the group members form a representive sample of all general field galaxies, it may be stated here that the results obtained seem to give an affirmative answer. In the present material there are 53 spiral systems above gal. lat. $+30°$ out to an absolute distance modulus of 30.0, which have altogether 82 physical companions with absolute pg magnitudes brighter than $M = -15.0$ (the observed number out to a separation of 50 kpc has been multiplied by 3.3; cf. the next section). On the other hand, the smoothed-out space density of galaxies brighter than $M = -15.0$ is about 0.17 per Mpc^3 (cf. sect. 14–15), which in the volume considered leads to a total number of approximately 180. Thus, over 70 % of all galaxies can be referred to the groups. Since the present investigation does not claim to be complete, it seems likely that the great majority of galaxies in the general field are members of physical groups of the type studied here. The conclusion is that the present material approximates to a random sample.

At this point some data will be presented for the three nearest and best-known groups of galaxies: the Milky Way group, the M31 group, and the M81 group. These physical groups, which in all respects appear to be comparable to the groups studied in the present paper, will later on be referred to for comparison. There does not seem to be any doubt that the Local Group is really two associations that happen to be located rather close together: one group around each of the two giant spiral galaxies (there may be some uncertainty as to the status of the two Ir I systems IC 1613 and Wolf–Lundmark–Melotte, which are exceptionally distant both from the Milky Way and from M31). The distances listed in Table 1 have been taken from the very detailed study of the Local Group by van den Bergh (1968), which is also the source for the absolute magnitudes and masses of SMC and LMC; the Capricornus system, not listed by van den Bergh, has been assumed to be at a distance <250 kpc on account of the high resolution. The remaining data are from my previous works (1958, 1964); the log. masses in brackets have been derived from absolute luminosities and integrated color indices by a relation given in the last-mentioned paper. The M81 group has been studied previously (Holmberg 1950). A new addition is Ho IX, a highly resolved Ir I system very close to M81 at $\alpha = 9^{\mathrm{h}}53^{\mathrm{m}}.5$, $\delta = +69°\ 16'$ (1950); the total pg magnitude has been measured on a Mount Wilson 60-inch plate.

Table 1 probably includes all group members outside the galactic absorption belt that are brighter than $M = -13.5$; those objects for which information on M is not listed (app. magnitude not accurately known) are all fainter than this limit. It may be noted that down to an absolute magnitude of $M = -9$ the three groups probably have more than 100 members (cf. the luminosity function derived in sect. 12). In spite of the incompleteness, the material available permits certain conclusions. We find that seven out of 22 members (IC 1613 and WLM not included) have separations from the central galaxy of less than 50 kpc; for the Milky Way group the separation is assumed to be equal to the distance multiplied by $\pi/4$, which is the average projection factor for a random orientation of the distance vectors. The arithmetical mean of the separations (21 members) amounts to 111 kpc, whereas the maximum separation is about 400 kpc.

Table 1. Data for members of the Local Group (=MW group+M31 group) and the M81 group.

Columns 2–6 give the number according to de Vaucouleurs *et al.* (1964), the adopted distance, the separation from the central galaxy, the abs. pg magnitude, and the log. mass (solar units).

Designation	Ref. Cat.	Distance	Separation	M	$\log \mathcal{M}$
Milky Way group					
Milky Way				—	11.1
NGC 6822		465 kpc	—	−15.3	9.1
SMC	A 51	60	—	−16.2	9.2
Sculptor	A 58	84	—	—	—
Fornax	A 237	188	—	—	—
LMC	A 524	50	—	−17.6	9.8
Leo I	A 1006	220	—	−10.8	—
Leo II	A 1111	220	—	− 9.1	—
Draco	A 1719	67	—	—	—
Capricornus	A 2144	< 250	—	—	—
Ursa Minor	—	67	—	—	—
M31 group					
NGC 224		690 kpc		−20.4	11.5
NGC 147		690	89 kpc	−14.2	(9.0)
NGC 185		690	85	−14.5	(9.2)
NGC 205		690	7	−15.9	(9.4)
NGC 221		690	5	−15.7	9.6
NGC 598		690	180	−18.4	10.6
IC 1613		740	>500	−14.5	8.6
WLM	A 2359	760	>500	−13.5	(7.6)
M81 group					
NGC 3031		2900 kpc		−19.8	11.2
NGC 2976		2900	71 kpc	−17.0	(9.7)
NGC 3034		2900	32	−18.5	(10.7)
NGC 3077		2900	40	−17.1	(9.9)
IC 2574		2900	155	−16.8	(8.9)
Ho I	A 936	2900	125	−14.4	(7.9)
Ho II	A 814	2900	425	−16.6	(8.9)
Ho IX	—	2900	9	−13.5	(7.6)

2. *Statistical approach to a study of physical groups*

In a previous paper (Holmberg 1940) the writer has used a special procedure, somewhat different from the method to be applied in this investigation, to study the grouping tendencies among galaxies. The analysis led to a statistical separation of physical and optical companions; the groups were revealed as they actually exist in space. In circular areas around presumptive central galaxies from the Shapley-Ames catalogue (1932) physical and optical companions were picked up, the material being supplied by the General Catalogue, as revised by Reinmuth (1926). If the radius of the survey areas is large enough, the statistical distribution of the observed separations can be dissected into two parts: one distribution corresponding to the background–foreground field and another referring to physical companions.

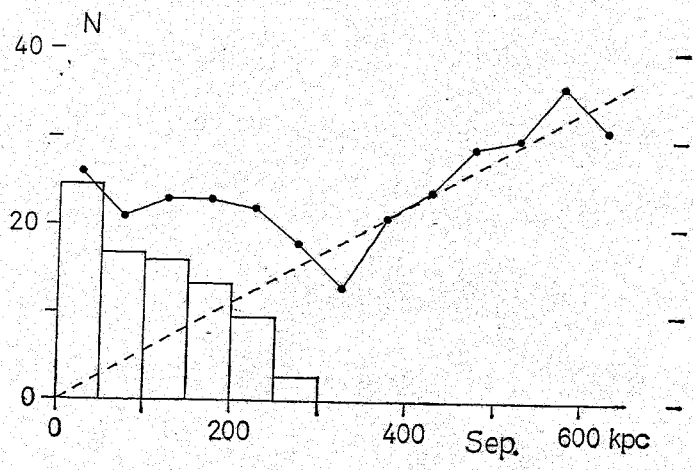

Fig. 1. Statistical distributions of separations, based on redshift distances, of physical and optical companions to 111 Shapley–Ames galaxies.

For Sh–A galaxies with $m = 12.1$–13.0 it was found that the mean separation of the latter companions amounts to 15′ and the maximum separation to about 50′.

By means of the redshifts available it is now possible to calibrate these results. The Reference Catalogue by de Vaucouleurs *et al.* (1964) and a subsequent list by the same authors (1967) give redshifts for 290 Sh–A galaxies with $m = 12.1$–13.0 (Virgo cluster area omitted); the mean redshift as reduced to the galactic center is 2150 km/sec. With a Hubble parameter $H = 80$ km/sec. per Mpc, the above mean separation corresponds to 118 kpc, and the maximum separation to about 400 kpc. Furthermore, 28 % of the physical companions have separations from the central galaxy of less than 50 kpc.

For the sake of completeness, the analysis will be repeated by using individual distances to the central galaxies, as derived from the redshifts. In the case of Sh–A galaxies with $m \leqslant 13.0$, gal. lat. $> +30°$, and $\delta > -20°$ (the limits of the previous material) redshifts above 1490 km/sec are available from the above sources for 111 objects outside the Virgo cluster area. In order to get a radius of the survey areas of at least 650 kpc, corresponding to the radius of 2° used in the previous analysis, it has been necessary to adopt this rather high redshift limit; the value of the redshift as a distance indicator is however improved. The resulting distributions of the separations of physical and optical companions in the 111 survey areas are shown in Fig. 1. The latter distribution is represented by a straight line, the inclination of which is based on the frequencies in the outer parts of the survey areas. The histogram refers to the physical companions, their total number amounting to 83. We find a mean separation for the latter of 110 kpc and a maximum separation of about 300 kpc; the relative number of physical companions with separations of less than 50 kpc is 30 %.

The above results have been given in some detail on account of their importance as a background to the subsequent analysis. To summarize, we have found mean separations of physical companions from the central galaxy of 111, 118, and 110 kpc, respectively, and maximum separations of 300–400 kpc; the relative frequency of companions with separations of less than 50 kpc amounts, on an average, to 30 %. It should be kept in mind that these results are of an empirical nature; the only assumption involved refers to the value adopted for the Hubble parameter.

The results found here, as well as the results of the following sections, are in disagreement with those derived by Zonn (1968) from a study of double galaxies on the Palomar Sky Atlas. The reason may be the rather complicated procedure used by Zonn and its dependence on a number of assumptions. On the other hand, the results agree with the conclusions by Swjagina (1966), also based on the Sky Atlas, that dwarf satellites accompany over 50 % of all galaxies.

Chapter II. Observation program

3. *Practical difficulties in the survey work*

The most serious difficulty encountered in studies of satellites is the problem of separating the physical companions from the optical ones, that is, from the background–foreground field. A decrease in the limiting magnitude by one magnitude class will increase the number of optical companions by a factor of 4, as will also a doubling of the radius of the survey area. In the analysis reported in the preceding section the difficulty was not of a serious nature on account of the rather bright limiting magnitude. The problem will be of another order of size when we try to pick out all dwarf satellites on the Palomar Sky Atlas. On account of the tremendous number of galaxies down to the limit of the Atlas, it is quite impossible to use the same type of survey area, with a radius that is considerably larger than the maximum separation of the satellites. In order to reduce the ratio of optical to physical companions, we have to be satisfied with rather small fields, including only those satellites that are comparatively close to the central galaxy. In the present work the practical limit has, as will be demonstrated later, been found to be survey areas with a radius of 50 kpc. According to the preceding section, areas of this size will include about 30 % of the total number of satellites. Still, the number of optical companions is in some cases uncomfortably large.

In order to determine empirically the number of optical companions, it is necessary with the above procedure to introduce comparison areas located at suitable distances from the survey area. With two fields, one on each side of the survey area, possible gradients in the distribution of galaxies are largely eliminated. If the three areas are of the same size, and if the galaxies are registered in exactly the same way, we ought to get a reliable measure, at least in a statistical sense, of the size of the background–foreground population.

It may be remarked that the successful separation of physical from optical companions ultimately depends on the difference in space density between the two groups. The final analysis of 160 satellite systems leads to a mean space density of satellites (in the volumes corresponding to survey areas with a radius of 50 kpc) of about 100 per Mpc^3, whereas the smoothed-out density in the general field amounts to only 0.17 per Mpc^3 (cf. sect. 14–15; for practical reasons, the densities refer to galaxies brighter than $M = -15.0$). There is thus a difference in density by a factor of about 600. For comparison, it may be noted that the Virgo cluster has a space density of about 20 per Mpc^3 (cf. sect. 13).

Another problem to be discussed is whether it is possible to identify on the Sky Atlas prints distant dwarf galaxies of low surface luminosity, objects that are comparable to some of the fainter members of the Local Group. The present survey is supposed to include dwarf satellites down to an absolute pg magnitude of about -10.6 (abs.

dist. mod. $\leqslant 30.0$) or down to -11.8 (mod. $\leqslant 31.2$), which with a galactic absorption of 0.3 magn. would mean a limiting apparent magnitude $\leqslant 19.7$. At the largest distances, the smallest dwarfs are found to have major diameters of about 0'.2, as measured on the blue prints, or about 0'.3, as reduced to the photometric diameter scale of Holmberg (1958). Practical experience shows that it is indeed feasible to pick up dwarf galaxies down to these limits. The reasons are (*a*) that the reproduction of the original Sky Atlas plates was aimed at preserving the faintest details at the limit of the plates (cf. Minkowski and Abell 1963), and (*b*) that the surface brightness of a galaxy is independent of the distance. The surface magnitude of the faintest dwarfs would in fact be more or less comparable to that of the Leo I system in the Local Group (cf. Table 1), which is a fairly outstanding object on the Sky Atlas prints. Even at a great distance, a system of this type would be readily recognizable if looked for in a very small survey area and studied through an eyepiece of adequate magnification.

It is interesting to find that it is possible to get valuable information on the dwarf satellites around distant spiral galaxies but very difficult, if at all possible, to make up a list of dwarf systems of the same absolute luminosity in the Local Group. The nearby dwarfs ought to be clearly visible on the Sky Atlas prints, but their distances are difficult to estimate (cf. van den Bergh 1966); the local systems cannot be separated from more distant galaxies. The position of the observer inside the Local Group is in this case a disadvantage.

A final question is, what kind of information can be acquired about the individual galaxies in the survey areas. Magnitudes would be of great value but cannot be measured for the faintest dwarf systems with present observational technique. Attempts to estimate magnitudes from the Sky Atlas prints would involve a great deal of work and would undoubtedly yield results of low accuracy. The diameters of the galaxies can, on the other hand, be readily measured down to about 0'.2. The morphological types can usually be estimated for the medium-sized and large galaxies. It will be shown that even information that is limited to diameters and types may be sufficient to obtain interesting results.

4. *Observation procedure*

The survey work refers to altogether 174 spiral galaxies of types So–Sa–Sb–Sc, both normal and barred spirals. The material comprises all systems of these types in my catalogue (Holmberg 1958) that have major diameters $\geqslant 5'.0$ (and distance moduli below certain limits). In order to get a more complete material, 38 galaxies with diameters above 5'.0 have been added from the Reference Catalogue by de Vaucouleurs *et al.* (1964; the diameters of this cat. have been reduced to the Holmberg diameter scale).

With respect to the following analyses it seemed advisable to divide the spiral systems into three different classes, *A*, *B* and *C*.

Class A. Systems with an edgewise orientation (app. diam. ratio $\leqslant 0.53$) that are not seriously disturbed by nearby large galaxies.

Class B. Systems with a face-on orientation (app. diam. ratio > 0.53) that are not seriously disturbed by nearby large galaxies.

Class C. Systems that may be disturbed by nearby large galaxies.

In the writer's diameter system, a diameter ratio of 0.53 corresponds to an inclination of the principal plane to the line of sight of about 30°. As regards the disturbance from another galaxy, we have to consider not only the gravitational action on the sat-

ellites of the primary galaxy but also a possible mix-up of the satellites belonging to the two systems. In an attempt to pick out spirals that are not seriously disturbed, we have tried to apply the following working rule, based on the separation of the second galaxy from the primary system, as compared to the radius, r, of the survey area. Separation $>2r$: no disturbance; $r<$sep.$<2r$: no disturbance if the estimated mass of the second galaxy is less than one-fifth of the mass of the primary system; sep. $<r$: no disturbance if the mass is less than one-twenty-fifth. The masses are estimated from the luminosities and morphological types (or integrated colors). Following this rule, the number of spiral systems in the classes A, B and C are found to be 62, 64 and 48, respectively.

The distance moduli of the spiral galaxies have been taken from the writer's catalogue (1964), which lists absolute moduli, as derived from both photometric data and redshifts ($H=80$); the arithmetical mean has been accepted (for four objects the moduli have been revised). In the case of the 38 galaxies from the Reference Catalogue, the distances are based only on the redshifts (all redshifts larger than 500 km/sec). As a limiting distance modulus we have adopted 31.2 for spirals with an edgewise orientation, and 30.9 for the remaining systems. The difference is due to the fact that the disturbance from optical companions is less pronounced for the former group, the physical companions apparently being confined to a position-angle interval of 30°–90° (cf. sect. 7). It may be noted that the number of optical companions in a survey area is, on an average, proportional to the distance.

The adopted absolute distance moduli, and the classes to which the galaxies have been assigned, are listed in Table 7.

It should be pointed out that the material includes some spiral systems from the Virgo cluster. As regards number of satellites, these spirals seem to be comparable to galaxies in the general field. The number of optical companions, as found from the comparison areas, also seems to be the same, which is explained by the fact that the great majority of the background objects are located far behind the cluster.

For the circular survey areas around the selected spirals we have, as was explained in the preceding section, chosen a radius of 50 kpc. The apparent radius ranges from 251′ (NGC 224) to 9′.9 (dist. mod. $=31.2$). The two comparison areas, of the same size, have been placed at standard distances of 100 mm east and west of the survey area, the distances being measured parallel to the edges of the Sky Atlas prints. For some nearby galaxies with very large survey areas the distances have been increased to ± 200 mm; in the few cases in which a comparison area happens to include a prominent galaxy, it has also been moved to twice the distance. For NGC 224 and 598, which for the sake of completeness have been included in the material, no comparison areas have been used, the number of optical companions in these cases presumably being $=0$.

Although the actual survey work on the Sky Atlas is based on the 103*a*-O prints a careful comparison has always been made between the blue and the red prints; the standing rule has been that no object is to be included unless it is recognizable as a galaxy on both prints. The work has been performed with an eyepiece having a magnification of 10 times, and equipped with a precision scale divided into 0.1-mm intervals.

The *first part* of the work was aimed at picking up all galaxies in the survey areas and the comparison areas that have major diameters ≥ 1.0 kpc (as referred to the distance adopted for the central spiral system). For a few very distant spirals this corresponds to an apparent diameter as small as 0′.20; on an average, the limiting diameter

is 0'.44. For all galaxies above this limit the major diameters have been measured. In the survey areas the polar co-ordinates have also been determined, that is, the separation of the object from the central system and the position angle, as measured from the direction of the major axis of the system. Attempts to estimate the morphological types have been successful only for galaxies larger than about 1'.0, and then only by a careful comparison of the blue and red atlas prints.

In the *second part* of the work, an attempt was made to extend the survey down to a limiting diameter of 0.61 kpc. Although the disturbance by the background–foreground field now becomes rather serious, it was found possible to do this for spiral systems with distance moduli $\leqslant 30.0$. The limiting apparent diameter is in this case about the same as above or 0'.21. The results of the second part will be used only to determine the statistical distribution of the absolute diameters of galaxies (cf. sect. 10).

5. *Results*

Some data referring to the number of survey fields, and the number of galaxies examined, are summarized in Table 2. In the survey areas there are altogether 1273 galaxies with diameters larger than the above limits, and in the comparison areas 2084. The entire material thus comprises 3357 galaxies distributed over 518 fields.

Fig. 2 gives the statistical distribution of the 174 survey areas, the areas being grouped according to the number of galaxies (diameter $\geqslant 1.0$ kpc). The number of companions, physical and optical, of the central spiral galaxies ranges from 0 to 13. The smooth curve represents the Poisson distribution corresponding to the same total number and the same arithmetical mean. As expected, the observed frequencies deviate from a random distribution. In order to reduce possible disturbances by distant clusters that may fall within the boundaries of the survey areas, it seemed advisable to exclude the 14 most populous areas—those with more than eight objects, or double the average number. The following analyses will be based on the 160 survey areas that have a maximum of eight galaxies. For the same reason, and as a compensation, the 28 most populous comparison areas have also been omitted. In the second part of the survey, down to a diameter of 0.61 kpc, we have excluded two additional survey areas with more than 15 galaxies, and the four most populous comparison areas.

The number of *physical* companions to the central spiral system in a survey area is, in a statistical sense, represented by the difference between the number of galaxies in this area and half the total number in the two comparison areas. However, the cen-

Table 2. Summary of observational data.

	Class *A*	Class *B*	Class *C*	All
Number of survey areas (number of galaxies)	62 (436)	64 (441)	48 (396)	174 (1273)
Number of comp. areas (number of galaxies)	122 (760)	126 (702)	96 (622)	344 (2084)
				518 (3357)

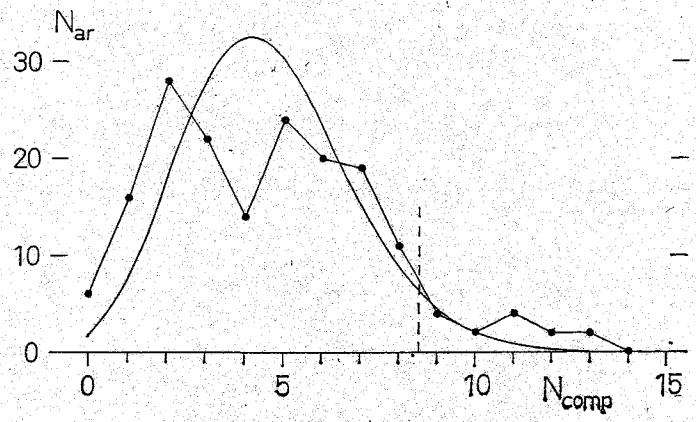

Fig. 2. Statistical distribution of 174 survey areas containing different number of galaxies. The smooth curve is the corresponding Poisson distribution.

tral systems, with a mean major diameter of 27 kpc, screen off parts of the survey areas, about 3 % (class *A*) and 5 % (class *B*). The comparison number is accordingly multiplied by 0.97 and 0.95, respectively (since for spirals of class *A* the physical companions are confined to position angles of 30°–90°, the factor will in reality be 0.65). For class *C*, comprising spiral systems of different inclinations which sometimes have large companions within the survey areas, the average factor is 0.95. It has been found that the accuracy is improved if the individual comparison number is replaced by the mean number derived from all the comparison areas as a function of the distance, the accidental fluctuations being reduced. The results listed in Table 7, as regards the number of physical companions (diam. $\geqslant 1.0$ kpc), are based on these smoothed-out comparison numbers. The values of N_{phys} range from -2 to $+7$, the estimated mean error of an individual number being about 1.2. It should be remarked here that the statistical distribution derived later for position angles, separations, and absolute diameters are based on the total number of optical companions, corresponding to all the comparison areas.

There does not seem to be any systematic dependence of the tabulated N_{phys} on the galactic latitude, which may indicate that the surface-brightness gradients in the outer parts of the satellites are so steep that the measured diameters are not seriously affected by galactic absorption. On the other hand, the results obtained in the extended survey (diam. $=0.6$–0.9 kpc) indicate a certain latitude effect, probably explained by the somewhat lower surface magnitude of these small satellites. For this reason, spiral systems with galactic latitudes below 29° (NGC 891, 925,1023, 1560, 2835, 7640) will not be included when the results of the extended survey are used in the determination of the distribution of absolute diameters (sect. 10).

It was stated above that survey areas with more than eight galaxies (diam. $\geqslant 1.0$ kpc) have been excluded, in order to reduce possible disturbances by background clusters. It is possible to make a check on the remaining part of the material by means of the charts of the distribution of distant clusters given in the catalogues by Zwicky *et al.* (1961, 1963, 1965, 1966, 1968). From the charts we estimate the fraction, f, of each survey area that is projected on a background cluster. If only clusters of a limited size are included, the very extended clouds being omitted, we find that $f=0$ for about half the number of survey areas; on an average, f amounts to 0.22. It is not possible to establish a statistically significant relation between N_{phys} and f, the coefficient of correlation being as small as $+0.10\pm0.10$ (m.e.).

For a reliable determination of the distribution of absolute diameters for galaxies in the physical groups it is important that the apparent diameter measures form a homogeneous system, that is, that the diameters are free from systematic errors that are a function of the diameter or of the distance modulus. All the diameters have been measured by the writer using the same eyepiece and taking care that the observing conditions were the same, for instance, as regards the illumination of the Atlas prints. A great part of the work has been repeated, with no indication of any serious changes in the diameter measures. The homogeneity is supported by the fact that N_{phys}, as listed in Table 7, shows no systematic dependence on the adopted distance modulus. Furthermore, an examination of the statistical distribution of the diameters of the galaxies in all the comparison areas shows that this distribution is compatible with the assumption of a constant space density of galaxies (cf. sect. 14). There is only a slight decrease in the number of galaxies with diameters less than 0.'35, which may be explained as a redshift effect in the diameters, since most of these small galaxies are at estimated distances of the order of 100–200 Mpc. It should be noted here that the diameters of the small physical satellites of the spiral systems do not suffer from any redshift effect; whereas most of the background objects are giant galaxies at very large distances, the satellites are dwarf systems with an average distance modulus of about 30.0.

6. *Colors of nuclei of spiral galaxies*

In view of the current discussion on the possibility of explosive events in the nuclear parts of spiral systems, resulting in the ejection of matter, it seemed important to look for indications in this direction in the analysis of the present material. Since calibrated pg and pv plates are available for most of the spiral galaxies of Table 7, we may as a starting-point try to collect some information regarding the nuclei of these systems. On account of the difficulty of defining the extension of a nucleus, no attempts will be made to determine apparent diameter or magnitude. The color index of the central part of the nucleus can however be easily measured.

Nuclear colors have been determined for altogether 172 spiral galaxies listed in my previous catalogue (Holmberg 1958). As a rule, 2 pg and 2 pv plates are available, taken with the Mount Wilson 60-inch or 100-inch telescope; the plates are calibrated by extrafocal exposures of stars. A number of galaxies could not be included, due to the fact that the nucleus is wholly or partly covered by absorption lanes; in a few cases, the central part of the nucleus is over-exposed. The measurements refer to a central cross-section along the minor axis of each galaxy, the derived color index being a mean result, corresponding to three points on either side of the center of the nucleus at distances of $\pm 2''$, $\pm 4''$ and $\pm 6''$; in the case of large nuclei, the distances have been increased to $4''$, $6''$ and $8''$. The colors have been corrected for selective galactic absorption by means of a relation derived by the writer in the above-mentioned paper, and for redshift effect ($-0^m.015$ per 10^3 km/sec); the latter correction is in the present case rather small. The mean error of a final color index (2+2 plates) amounts to $0^m.045$, as found from the internal agreement.

The nuclear part of a spiral system is apparently free from absorbing matter, the color index showing no systematic dependence on the apparent diameter ratio as long as this ratio is larger than 0.52, corresponding to an inclination of about 30° of the principal plane to the line of sight (absorbing matter could however be present, if it is assumed to have a spherical distribution). For diameter ratios smaller than 0.52

Table 3. Mean pg–pv color indices, corrected for galactic absorption and redshift effect, for the nuclei of spiral galaxies of different types.

Type	Number	$\bar{C}$	Disp.
Sc+	21	$+0^m.38$	$0^m.093$
Sc−	45	0.62	0.108
Sb+	21	0.74	0.093
Sb−, Sa	20	0.76	0.092
So	19	0.77	0.064

the color index increases, indicating that the nuclear part, although no absorption lanes are visible across the nucleus, is being covered by obscuring matter located in the outer parts of the system.

Table 3 gives the mean pg–pv colors for different types of galaxies, and the dispersions of the individual values around the means; the results are based on galaxies with diameter ratios larger than 0.52. As the type changes from Sc+ to So, the color index gradually increases from $+0^m.38$ to $+0^m.77$; the latter color happens to be the same as the mean integrated color previously derived by the writer (1958) for elliptical galaxies.

In Table 7 the nuclear color *excess*, ΔC_N, or the difference between observed color and mean color, as given in Table 3, is listed for 110 galaxies. For those objects that have diameter ratios $\leqslant 0.52$, a correction for internal absorption (as derived from the material) has been applied; in a few exceptional cases this correction may be as large as $-0^m.15$.

It is naturally of the greatest interest to study the nuclear colors in those cases in which the spectrum indicates an unusual activity in the nuclear region or in which the nucleus in other ways appears to be peculiar. Unfortunately, the present material includes only two Seyfert galaxies, NGC 4051 and 4258; they both have large negative color excesses, $-0^m.11$ and $-0^m.09$, respectively. From an inspection of the Hubble plate collection, Sérsic and Pastoriza (1967) have selected 20 galaxies that appear to have abnormal nuclei; it is a very interesting fact that the list comprises only barred spirals. The present material includes eight of these galaxies, their mean nuclear color excess amounting to $-0^m.06$. The presence of the emission line $\lambda 3727$ (*O* II) in the spectrum also seems to affect the nuclear color. When this line is present in measurable strength in the nuclear region, as indicated in the redshift catalogue by Humason *et al.* (1956), the mean color excess is $-0^m.03$; when the line is not present, the mean excess is $+0^m.03$.

In conclusion, it should be remarked that there is a fairly pronounced correlation between the nuclear color index and the spectral class, as listed by Humason in the redshift catalogue. In those cases in which the spectrograph slit has been put across the nucleus, the spectral classification apparently refers to the nuclear part of the galaxy. The linear regression line gives a mean color index of $0^m.44$ for F0, $0^m.57$ for F5, $0^m.70$ for G0, and $0^m.82$ for G5, the dispersion in the residuals being $0^m.087$. There is also a correlation between the nuclear color excess, as defined here, and the deviation of the observed spectrum from the mean spectral class corresponding to the morphological type. The good agreement indicates that the data available on nuclear colors and spectra form a consistent system.

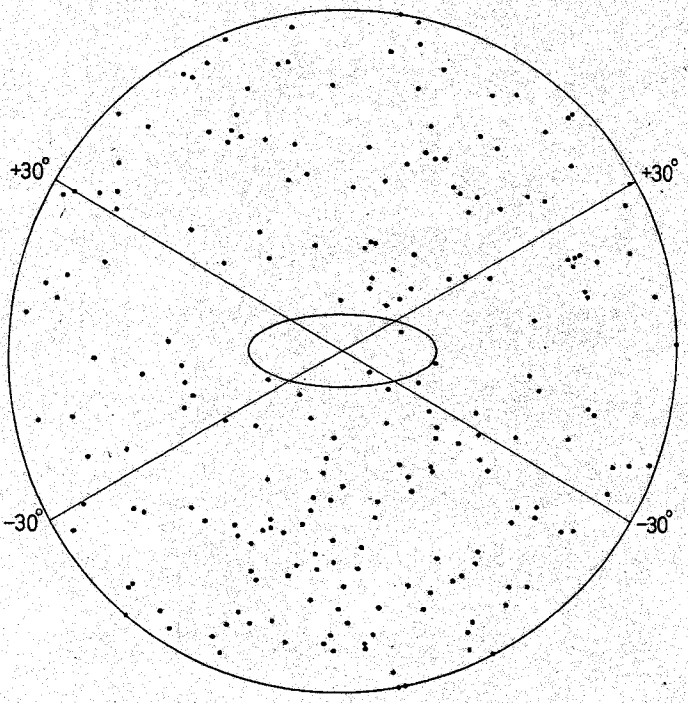

Fig. 3. Combined distribution of 218 galaxies in 58 survey areas around spiral systems of class *A* (edgewise orientation). The ellipse shows the average size of the central system.

Chapter III. Analysis of results

7. *Distributions of position angles and separations*

As stated above, we have determined for all the galaxies (diam. $\geqslant 1.0$ kpc) in the survey areas the separation from the central spiral system and the position angle as measured from the direction of the major axis of the system. It may be recollected that 14 survey areas with more than eight galaxies have been excluded; the remaining material refers to 160 survey areas.

The map in Fig. 3 gives the combined distribution over the survey area (radius = 50 kpc) of 218 physical and optical companions belonging to the 58 spiral systems of class *A* (edgewise orientation; no disturbance from the outside). The ellipse shows the average size and shape of the central galaxy, whereas the straight lines represent position angles of $\pm 30°$. An examination of the figure indicates, quite unexpectedly, that the position-angle interval between $-30°$ and $+30°$ is under-represented, most of the companions being located in the remaining part of the area.

The statistical distribution of the position angles, as derived from the same material, is reproduced in Fig. 4 (upper part); the frequencies refer to 15° intervals of the position angle φ. The broken line represents the distribution corresponding to the optical companions alone, the position angles of which are assumed to be distributed at random. There are in all the comparison areas referring to the 58 class-*A* systems a total of 300 galaxies; if this number is divided by 2 and multiplied by 0.97 (cf. sect. 5), we arrive at 24.2 optical companions in each position-angle class. The conclusion seems to be that all galaxies of the interval 0°–30° are optical companions, the physical companions being concentrated in the interval 31°–90°. The total number of physical companions, in all about 74, is represented by the area between the full distribution curve and the broken line.

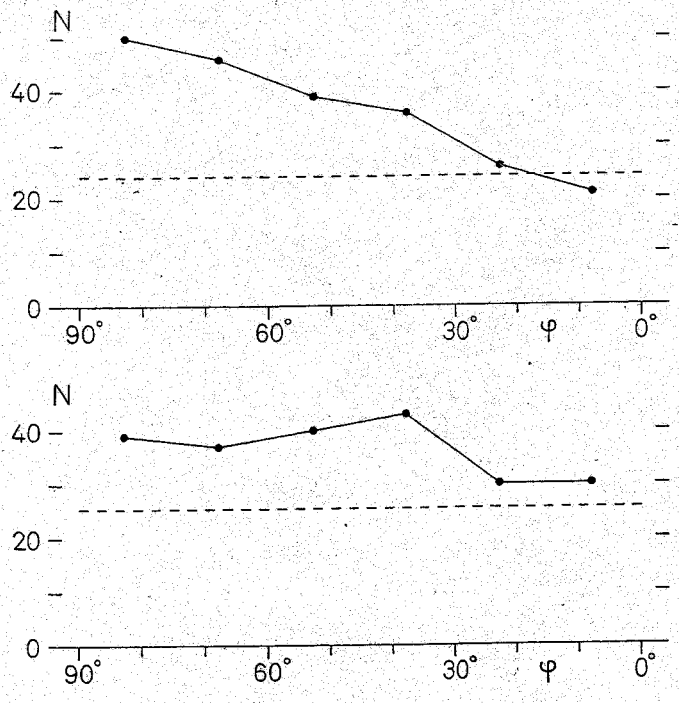

Fig. 4. Statistical distributions of position angles of companions to spirals of class A (upper part), and spirals of class B (lower part). The broken lines refer to optical companions.

On account of the peculiar distribution in position angle, we have, in determining the number of physical companions to individual spirals of class A (Table 7), included only those companions that have position angles larger than 30°. The comparison number referring to optical companions has been multiplied by $2/3 \cdot 0.97 = 0.65$.

The distribution of the position angles of 219 physical and optical companions belonging to the 57 spiral systems of class B (face-on orientation; no disturbance from the outside) is shown in the lower part of Fig. 4. Half the total number of optical companions, as found in the comparison areas, is now multiplied by 0.95 (cf. sect. 5); the resulting number of optical companions per position angle class is 25.6. In this case, the distribution referring to the physical companions deviates only to a small extent from a random one. The total number of physical companions is about 65.

Since the excess of large position angles found for satellites belonging to spirals with an edgewise orientation may be an important feature, it would be of interest if it could be confirmed by material from other sources. A possibility for a check is offered by the catalogues of galaxies, presumably complete down to $m = 15.5$, published by Zwicky and collaborators (1961, 1963, 1965, 1966, 1968). From these lists we have picked out all galaxies of types So–Sa–Sb–Sc outside the Virgo cluster area that have apparent magnitudes $m < 12.0$ (types and magnitudes from Humason *et al.* 1956 and Holmberg 1958), and apparent diameter ratios $b/a < 0.50$ (diameters and position angles of major axes from Reinmuth 1926). In circular survey areas with a radius of 30′ around these galaxies, in all 72 (areas with more than one galaxy brighter than $m = 12.0$ being omitted), there are 140 companions listed in the catalogues. An examination shows that the number of companions with position angle φ larger than 30° is 3.4 times the number corresponding to $\varphi = 0° - 30°$. If the radius of the areas is reduced to 15′ the ratio is increased to 4.2. In both cases the number in the interval $\varphi = 0° - 30°$ closely agrees with the expected number of optical companions. Although the limiting magnitude is rather bright, and the number of physical satellites correspond-

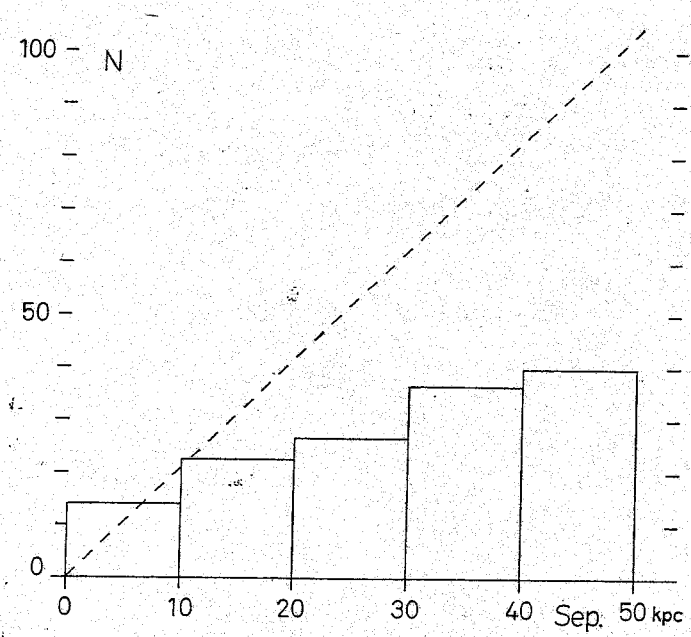

Fig. 5. Statistical distributions of separations of physical companions (histogram) and optical companions (broken line) from the central spiral systems.

ingly small, this simplified analysis thus confirms the above result. It should be noted that the analysis is based on an entirely different material.

The distribution of the position angles seems to indicate that nearby satellites of spiral systems avoid local latitudes below 30°. It may be noted that the same distribution is found for the satellites of the Milky Way and M31 (Table 1), the only exception being the very distant NGC 6822 (the M81 group is disturbed by the rather massive system M82). In the search for a possible explanation, it may first be pointed out that the surfaces of equal gravitational potential around a flattened spiral system are not spherical; it seems difficult, however, to estimate the resulting effect on the motions of the satellites. Secondly, many spirals are apparently surrounded by hydrogen clouds, which in the principal planes of the galaxies may extend far beyond the optical boundaries. The friction produced by the gas is perhaps sufficient to retard the motions of nearby satellites in low latitudes. If the gas clouds contain absorbing matter, which seems unlikely, some of the satellites may be obscured. On the other hand, the satellites are distributed in the way we should expect, if they are formed by matter ejected from the nuclear part of the spiral. In low latitudes, the ejection may be stopped by the gas located in the main body of the system; this seems to be the case in M82. The discussion on the origin of the satellites is continued in the next two sections.

The separations measured for all the galaxies (diam. $\geqslant 1.0$ kpc) in the survey areas extend from a few kpc to 50 kpc. In Fig. 5, the histogram gives the statistical distribution of the separations of physical satellites from spiral systems of classes *A* and *B*; the total number is about 139. The broken line represents the distribution of optical companions, which is assumed to be a random one; according to the above analysis, the total number of these companions is about 250. The former distribution is obtained if the numbers corresponding to the latter distribution are subtracted from the total numbers in the survey areas referring to the different separation intervals.

It is quite apparent from the figure that it would not serve any useful purpose to try to extend the survey work to separations above 50 kpc. Whereas for small separations the ratio of physical companions to *all* companions is quite favorable, it is re-

duced in the interval 41–50 kpc to 31 %. For still larger separations the ratio would decrease rapidly, since the number of optical companions is steadily increasing; on the other hand, the distribution of physical companions may have a maximum at a separation of 40–50 kpc, as is indicated by a comparison of Fig. 5 with Fig. 1. An extension of the work to larger separations is possible only if the diameter limit adopted for the galaxies, in the present case 1.0 kpc, is increased.

It may be of interest to mention that a study of the present material does not indicate any systematic dependence of the size of the satellites on the separation from the central galaxy. The separation interval is perhaps too limited to permit the determination of a possible correlation of this type.

The analyses of this and the two following sections do not include spiral systems of class *C* (disturbance from the outside), since the satellites of the primary galaxy may be mixed up with satellites belonging to other nearby galaxies.

8. *Number of satellites and nuclear color of central galaxy*

As was described in sect. 6, the nuclear pg–pv color indices have been determined for the majority of the central spiral systems. The nuclear color excesses, as obtained by subtracting the mean colors of Table 3, are listed in Table 7. The color excesses range from $-0^m.23$ to $+0^m.24$.

It was found above that the nuclear color excess is negative in those cases in which the spectrum or a direct inspection of plates indicates an unusual activity in the nuclear region. On account of the possibility of explosive events in such nuclei, it seemed of interest to examine whether the number of physical satellites of a spiral system is in any way related to the nuclear color or to the nuclear color excess.

The upper part of Fig. 6 shows the dependence of N_{phys}, as listed in Table 7, on the nuclear color index. The plot refers to the spiral systems of classes *A*–*B* with known colors, in all 72; the number of physical companions, ranging from -2 to $+5$, also

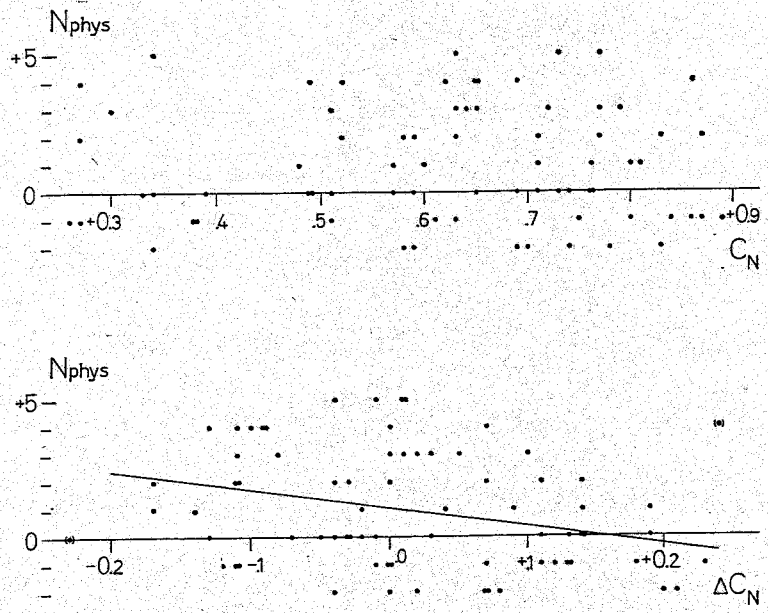

Fig. 6. Variation in number of satellites with nuclear color index of central galaxy (upper part), and with nuclear color excess (lower part).

totals 72. A study of the figure shows, quite conclusively, that there is no indication of any systematic variation in N_{phys} with C_N.

Conditions are somewhat different, when N_{phys} is plotted against the nuclear color excess ΔC_N: a correlation seems to be indicated. About one-third of the spirals, those with color excesses larger than $+0^m.06$, have a mean number of satellites equal to 0.0; for the remainder the mean number is +1.5. If two spirals with exceptional color excesses are omitted, the coefficient of correlation amounts to -0.31 ± 0.11. Since the coefficient is almost three times the mean error, the result is supposedly significant. The straight line represents the regression line.

It is naturally tempting to try to interpret this result as indicating that the satellites have been formed from matter, presumably gas, ejected from the nuclear regions of the spiral systems. It should however be pointed out that it is possible to determine the morphological types of satellites with diameters above 2.5 kpc, and that no correlation exists between these types and the nuclear color excess of the central galaxy; for all values of ΔC_N there is a mixture of all types from E–So to Ir I. Even without knowing anything about the process by which the gas may be condensed into satellites, we would have expected such a correlation if the suggested interpretation were correct. The material at hand does not seem to offer any other possible explanation.

9. *Number of satellites and mass of central galaxy*

It seems natural to assume that the number of physical satellites must be a function of the size of the central galaxy or of some other parameter that is related to the size. In this section, the dependence of N_{phys} on total mass, hydrogen mass, and other absolute characteristics will be examined.

The total mass, and the HI mass, can be estimated from the absolute luminosity and the integrated color index (or the morphological type); in the present case, certain relations previously derived by the writer (1964) have been used. For a number of nearby galaxies direct observational results are available. The total masses for the majority of the spiral systems of Table 7 have already been listed in the above-mentioned paper. For the 38 spirals included from the Reference Catalogue the apparent magnitudes needed have been assembled from various sources, in the first place from the catalogue by Humason *et al.* (1956).

In the upper part of Fig. 7 the number of physical companions has been plotted against the log. total mass (solar units), the material comprising 113 spiral systems of classes *A–B* in Table 7 (two objects omitted on account of missing data). The log. mass ranges from 8.7 (NGC 4236) to 12.1 (NGC 4594). Quite unexpectedly, the plot does not indicate any correlation between the two parameters. The negative result may possibly be due to the fact that the separations of the satellites are limited to 50 kpc. It seems possible that the more massive spiral galaxies have satellite clouds of larger extensions than the less massive ones.

In the middle part of the figure, N_{phys} for the same material is plotted against the log. HI mass (solar units); the hydrogen mass ranges from 8.3 to 10.3 in the logarithmic scale. In this case a correlation is indicated, as represented by the straight regression line. The number of satellites approaches zero as the log. mass decreases below 9.0.

As was mentioned in the preceding section, spiral systems with nuclear color excesses larger than $+0^m.06$ have a mean number of satellites $=0.0$. The correlation

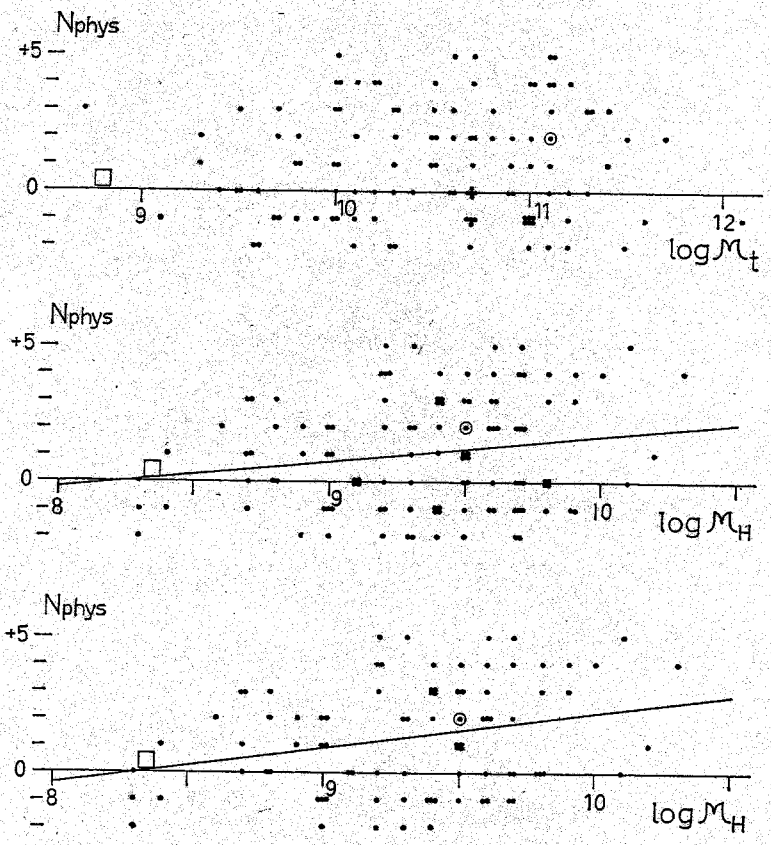

Fig. 7. Variation in number of satellites with total mass and HI mass of central galaxy (in the bottom part spirals with nuclear color excess $> +0^m.06$ are omitted). The square represents the mean result referring to 8 central galaxies of type Ir I.

found above is naturally reduced by the presence of these systems in the material. If the 26 spirals with high color excesses are left out, we arrive at the diagram in the lower part of Fig. 7. The coefficient of correlation now amounts to $+0.28 \pm 0.10$; since the result is about three times the mean error, it is presumably significant.

The open circle introduced in the three diagrams shows the position of the Milky Way (two nearby companions). The square gives the mean position referring to eight galaxies of type Ir I (NGC 1156–2366–3109–4532–6822, IC 1613, Ho II, WLM). In circular survey areas with a radius of 50 kpc around these galaxies a total number of three physical satellites have been found by applying the same procedure as that used for the spiral systems. Since the number does not significantly differ from zero, it seems likely that Ir I galaxies do not possess any physical satellites.

As regards other absolute characteristics of the spiral systems, there are weak correlations between N_{phys}, on the one hand, and absolute magnitude, absolute diameter, and morphological type, on the other. All these correlations are very likely reflections of the relation between N_{phys} and hydrogen mass.

To summarize the results of this chapter, it is recollected that physical satellites of spiral galaxies are apparently concentrated in high local latitudes, and that they seem to favor systems which have nuclear color excesses below a certain limit and which contain large amounts of gas. The results seemingly point to one interpretation: that the satellites have been formed from gas ejected from the central galaxies. This interpretation must be considered as a hypothesis, since the statistical evidence presented is not of a conclusive nature.

As regards possible ejections of matter, definitive results have been obtained from direct observations of explosive events in the nuclei of a number of systems, in the first place, some well-known Seyfert galaxies. In M82 (Lynds and Sandage 1963; Solinger 1969), and in NGC 1275 (Burbidge and Burbidge 1965), observational evidence shows that material has been ejected to great distances from the nuclei. In NGC 1068 (Walker 1968 *a*) nuclear clouds are being expelled at velocities that are probably in excess of the escape velocity; similar processes are apparently also taking place in NGC 4151 and NGC 7469. Nuclear clouds of the same type appear in the central region of the elliptical galaxy M87 (Walker 1968 *b*), indicating that the cloud-ejection process is not confined to spiral galaxies. Several attempts have been made to show that the ejected matter condenses into galaxies; references may be made to Arp (1967, 1968 *a*, 1968 *b*), and to Sérsic (1968). So far these attempts, which are based on statistical analyses of available data, have not yielded any results that appear to be conclusive. From a theoretical point of view, the construction of a model for the condensation process seems to encounter serious difficulties. In any case, if the velocity of the ejected gas is larger than the escape velocity, which often seems to be the case, possible condensations cannot give birth to gravitationally bound satellites.

While awaiting the accumulation of further observational data that may eventually lead to a settlement of the question, the conservative position to adopt for the present is naturally to assume that all the members of a physical group of galaxies have been formed more or less simultaneously from different parts of the same gas cloud. The formation of galaxies would thus be a parallel to the formation of stars in associations. In a previous investigation on the evolution of galaxies the writer (1964) has presented some arguments in favor of the assumption that all galaxies have approximately the same actual age.

Chapter IV. Distributions of absolute diameters and magnitudes

10. Distribution of logarithmic diameter

Before studying the statistical distribution of the log. absolute major diameters of the members of the physical groups, we shall reduce the apparent diameters, as measured on the blue Sky Atlas prints, to the writer's photometric diameter system. This system, which is defined by the diameters listed for 300 galaxies in Holmberg (1958), is based on a homogeneous plate material from the Mount Wilson 60-inch and 100-inch telescopes, and refers to a pg isophote of about $26^m.5$ per square second. A comparison of the Sky Atlas diameters with the photometric diameters indicates that the latter are, on an average, 1.46 times larger. The correction factor naturally depends to a certain extent on the type and the surface magnitude of the galaxy; for the smallest objects the factor can be determined only by extrapolation. However, if all log. diameters, as derived from the Sky Atlas, are increased by the same amount or 0.16, the internal consistency of the diameter system will remain unchanged. For most of the larger galaxies to be included in the analysis of the diameter distribution, the diameters can be taken directly from the writer's catalogue.

The statistical distribution of the log. major diameters, log A, of all the satellites in the 160 groups referring to spiral systems of classes A, B and C is given in Table 4. By the above correction, the limiting absolute diameter (in the extended survey with distance moduli $\leqslant 30.0$) has been increased from 0.61 to 0.89 kpc, corresponding

Table 4. Statistical distribution of log. absolute major diameter, log A (pc), as derived for the physical companions in 160 survey areas.

Columns 2–5 give the mean absolute pg magnitude (cf. Fig. 9), the total number of objects in the survey areas, the number of optical companions to be expected (as found from the comparison areas), and the resulting number (with mean error) of physical companions.

log A	$\overline{M}_{pg}$	N_{tot}	N_{opt}	N_{phys}
2.95–3.15	−11.16	363[a]	0.413·760[a]	49[a] ±11.4
3.15–3.35	−12.36	367	0.425·675	80 11.0
3.35–3.55	−13.56	122	0.425·169	50 5.5
3.55–3.75	−14.76	48	0.425· 43	30 2.8
3.75–3.95	−15.96	25	0.425· 10.8	20.4 1.4
3.95–4.15	−17.16	24	0.425· 2.7	22.9 0.7
4.15–4.35	−18.36	14	0.425· 0.7	13.7 —
4.35–4.55	−19.56	7	0.425· 0.2	6.9 —
4.55–4.75	−20.76	1	0.425· 0.0	1.0 —

[a] Only galaxies with $m-M \leqslant 30.0$ (57 survey areas); the frequencies should be multiplied by 2.92.

to a log. diameter (pc) of 2.95. The absolute magnitudes contained in the second column of the table will be explained in the next section. The third column gives for successive classes of log A the total number of physical and optical companions in the 160 (57) survey areas (class A: pos. angles $>30°$; cf. sect.7). The number (slightly smoothed out) of optical companions, as derived from all the comparison areas, is listed in the fourth column. It may be recollected that this number should be multiplied by the factor 0.65/2 (class A), or 0.95/2 (class B–C); the mean factor amounts to 0.413 in the first diameter class, and to 0.425 in the remaining classes. The resulting number of physical satellites, in all 274, appears in the last column. The mean error listed reflects the accidental fluctuations in the number of optical companions; it has been derived from the square root of this number.

It should be pointed out here that the central spiral systems have *not* been included in the analysis. Since all the survey areas are centered on prominent galaxies, the inclusion of these would lead to a serious over-representation of objects with large diameters. The correct procedure would be to include those galaxies which would fall within the survey fields, if these fields were distributed at random over the sky. The total area covered by all the fields amounts to about 70 square degrees (the large fields of NGC 224 and 598 being omitted), corresponding to approximately 0.4 % of the area covered by the Sky Atlas outside the galactic belt. A random distribution of the survey fields would thus include less than one of the 160 spiral systems.

In the first diameter class, log $A = 2.95 - 3.15$, the value found for N_{phys} must be multiplied by a certain factor in order to be comparable to the other class frequencies. The 57 survey areas with distance moduli $\leqslant 30.0$ contain altogether 77 physical satellites with log. diameters larger than 3.15, whereas the corresponding number in all the 160 areas is 225; the factor is $225/77 = 2.92$. In the first class N_{phys} is thus increased to 143 ± 33. As is clear from the large relative size of the mean error, the disturbance from optical companions is considerable in this class, indicating that attempts to pursue the survey work to still smaller satellites would not be successful.

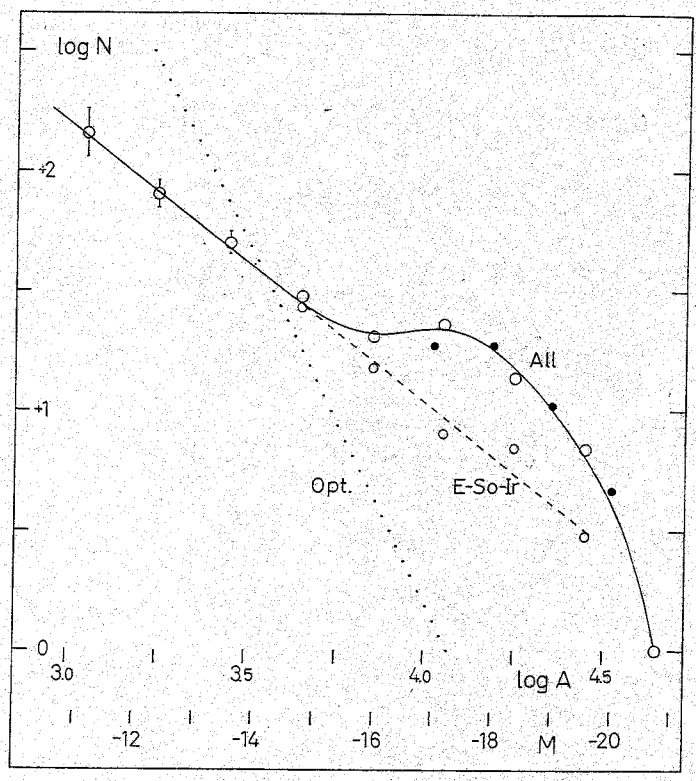

Fig. 8. Statistical distribution of log. absolute diameter (and absolute pg magnitude), as obtained for 274 satellites in 160 survey areas. The large open circles refer to the entire material, and the small circles to types E–So–Ir; the filled circles represent those satellites for which the absolute magnitudes are based on available apparent magnitudes.

The statistical distribution of log A is reproduced in Fig. 8 on a logarithmic scale. The large open circles (vertical bar = twice the mean error) represent the above class frequencies, whereas the full curve is supposed to give the smoothed-out distribution. In the direction of small diameters there is a steady linear increase in the logarithmic curve, no turning point being indicated, although the material includes diameters down to about 900 pc. On the other hand, there seems to be an unexpected maximum in the distribution for diameters of about 10 kpc. The dotted line represents the distribution of the subtracted optical companions.

For the medium-sized and large satellites it is possible to determine the morphological types. A division of the material in two type groups, E–So–Ir and Sa–Sb–Sc, leads to the very interesting result that the distribution corresponding to the former group, as represented by the small open circles, can be described by a straight line that is an extrapolation of the linear part of the total distribution curve. The region between the full curve and the broken line refers to the Sa–Sb–Sc group. The results indicate that there is, as has been suspected before, a definite lower limit for the diameters of Sa–Sb–Sc spirals, about 5 kpc on the present diameter scale, and that the linear part of the distribution curve in its entire length refers to galaxies of types E–So–Ir. The distribution curves will be further discussed in the next two sections.

11. Correlation between absolute magnitude and diameter

Although the diameter distribution leads to important conclusions, it would naturally be of greater interest to have access to the distribution of absolute magnitude.

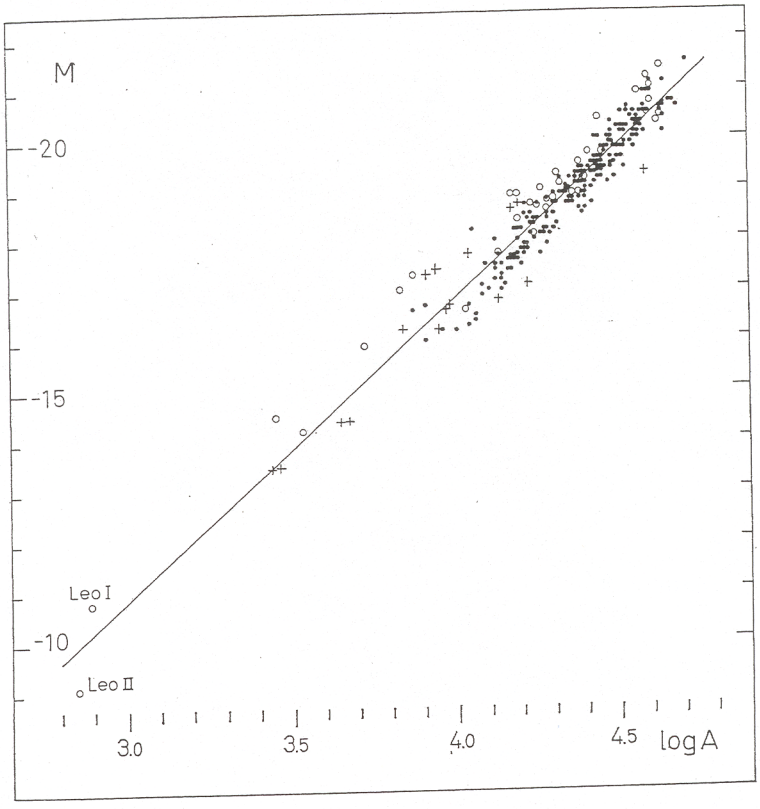

Fig. 9. Relation between absolute pg magnitude and log. absolute major diameter (pc) as obtained from the Holmberg (1964) catalogue for galaxies of types E–So (open circles), Sa–Sb–Sc (filled circles), and Ir I (crosses).

It seems possible to derive this distribution by an indirect procedure, without any knowledge of the magnitudes of the individual satellites.

In a previous investigation on the evolution of galaxies the writer (1964) has found pronounced relations between different galaxian characteristics. A study of the absolute pg magnitudes and log. absolute diameters, as listed in this paper, leads to the correlation diagram reproduced in Fig. 9. The diagram is based on 189 galaxies of types Sa–Sb–Sc, 36 of types E–So, 16 of type Ir I, and 5 of type Ir II, in all 246 objects. In order to facilitate comparisons with other results, the magnitudes have not been corrected for internal absorption, with the exception of the group Sa–Sb–Sc, for which *differential* absorption corrections have been applied. If the absorption-free magnitudes, as listed for the latter objects, are corrected by +1.0 magn. (Sa–Sb), or +0.7 magn. (Sc), they are reduced to a random orientation of the spirals with respect to the line of sight (the 5 Ir II objects have been treated as Sa–Sb spirals). The absolute magnitudes range from −9 and −11 (Leo I and Leo II, not included in the previous paper) to −21.5, and the absolute diameters from 0.7 to 50 kpc. The material thus covers the entire diameter range of the satellite population studied here.

The relation is very pronounced, and apparently linear, the coefficient of correlation being -0.962 ± 0.005. The regression line reproduced in the figure has the equation:

$$M = -6.00 \log A + 7.14. \qquad (1)$$

The relation indicates that the surface magnitude gets fainter with decreasing size, the total variation being about two magnitudes from the largest galaxies to the smal-

lest dwarfs. The dispersion of M around the regression line amounts to only 0.40 magn. On account of the accidental errors to be expected in the adopted distance moduli (and in the diameters) the final mean error in M, as derived from eq. (1), is estimated at 0.7 magn. It is of special interest that the different type groups of galaxies do not show any significant systematic deviations from the regression line; the only exception is the E–So group, with a deviation of about -0.3 magn.

By means of the above relation, the diameter distribution can be transformed to a distribution of absolute magnitude. In Fig. 8, the only change to be made is the replacement of the log. diameter scale by a magnitude scale. The absolute pg magnitude extends from -10.6, corresponding to the smallest diameter, up to -22.0, which seems to be the upper luminosity limit. The mean absolute magnitudes in the successive diameter classes are listed in the second column of Table 4.

The accuracy attained in the transformation process can be checked, for instance, by using the diameters and magnitudes available for the 160 central spiral systems. A comparison of the luminosity distribution, as derived from the diameters, with the same distribution obtained directly from the magnitudes indicates a very good agreement. A more conclusive check can be made by trying to determine the brighter end of the distribution curve in Fig. 8 directly from magnitudes. If we limit ourselves to luminosities higher than $M = -16.5$, an interval in which the disturbance from optical companions can be neglected, we find that magnitudes from the writer's catalogue are available for about two-thirds of the satellite population; magnitudes for the remainder can be obtained from other sources, in the first place, the catalogues by Zwicky *et al.* (1961, 1963, 1965, 1966, 1968). The distribution of the magnitudes for the 45 satellites brighter than $M = -16.5$ is given by the filled circles in Fig. 8. Considering the heterogeneity of the magnitude material, the points agree in a very satisfactory way with the adopted curve.

12. The luminosity function

As is found from Fig. 8, the logarithmic distribution of the absolute pg magnitudes of galaxies of types E–So–Ir can be described by a straight line extending from the lower limit $M = -10.6$ to about $M = -20$; in the interval -20 to -22 the curve falls off rapidly. The magnitude distribution for the Sa–Sb–Sc group is represented by a bell-shaped curve, extending from about $M = -15$ to $M = -22$.

It is a very interesting fact that the luminosity function derived for the E–So–Ir group agrees with the curve suggested by Zwicky (1957, 1964) for the members of galaxy clusters. The dense clusters may possibly have populations that are comparable to the E–So–Ir population studied here; in any case, these clusters are practically free from Sa–Sb–Sc spirals. The agreement also extends to the inclination of the log. distribution line. A least-squares solution, based on the eight class frequencies that define the linear part of the distribution in Fig. 8, gives an inclination of 0.195 ± 0.007, a result that within the limits of the accidental errors agrees with Zwicky's coefficient of 0.2. In a recent investigation of the luminosity function of elliptical galaxies in the Virgo cluster, Abell and Eastmond (1968) have arrived at a curve of the same type and the same inclination (0.2). In earlier studies of some dense clusters (all members included) Abell (1962, 1964) has found inclination coefficients that are slightly larger.

It may be pointed out here that the shape and the inclination of the linear distribution curve are not affected by the disturbance to be expected from the accidental errors in the absolute magnitudes (or absolute diameters). However, in accordance

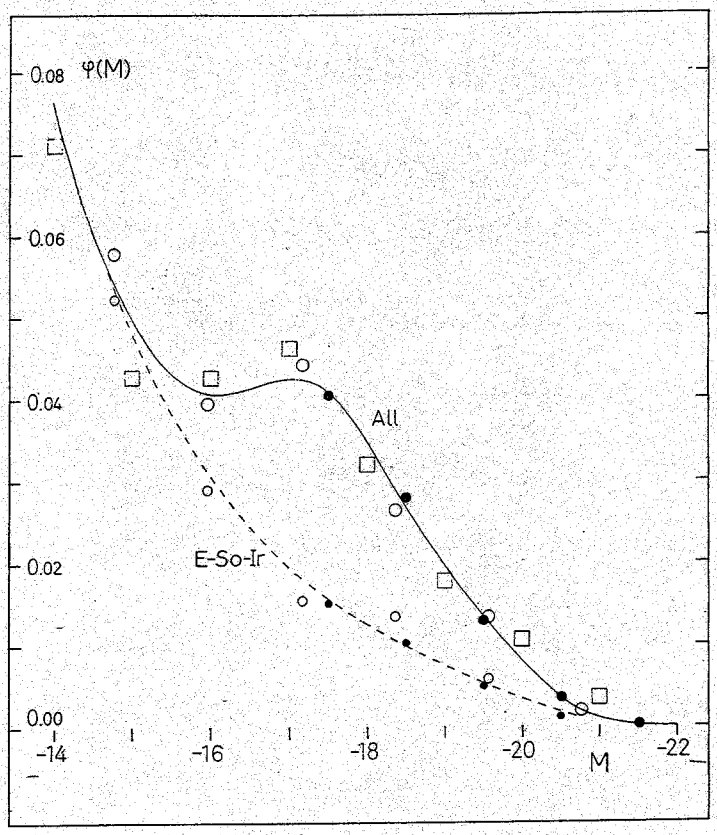

Fig. 10. The brighter end of the luminosity functions (corresponding to the right-hand half of Fig. 8), as calibrated for 1 Mpc³. The filled circles give the distributions derived for galaxies with known redshifts north of gal. lat +30°. The squares refer to the Local Group and the M81 group.

with well-known relations of stellar statistics, the curve should be corrected by a displacement towards fainter magnitudes by the amount $\Delta M = 0.195\,\varepsilon^2/2 \log e$, where ε is the mean error of M; if the error is 0.7 magn., as suggested above, the displacement would be $\Delta M = +0.11$. On the other hand, it was found in the preceding section that the absolute magnitudes of E–So galaxies, as derived by means of eq. (1), would be about 0.3 magn. too faint. Since, as far as can be ascertained from the present material, galaxies of these types make up 50–60 % of all objects in the E–So–Ir group, the average systematic correction to the absolute magnitudes would approximately neutralize the disturbance caused by the accidental magnitude errors. The distribution curve will be accepted without any corrections.

With a good degree of approximation the distribution referring to the Sa–Sb–Sc spirals, in all 35, can be described by a normal error-curve with a mean absolute pg magnitude of −17.7 and a dispersion of 1.2 magn. The accidental magnitude errors will not affect the mean but will to some extent increase the dispersion. Since the results are based on comparatively small class frequencies, and since the right-hand half of the observed curve happens to agree well with the curve derived from galaxies of known redshifts, as will be shown below, no corrections have been applied. It is interesting to recollect that, except for a systematic displacement in magnitude, the distribution agrees rather nicely with the classical luminosity function derived by Hubble (1936) from a study of the brightest resolved stars in nearby galaxies; Hubble's material referred mainly to Sc and Sb spirals.

In order to make possible a more detailed study, the distributions referring to the more luminous magnitude classes have been reproduced in Fig. 10. The full curve

(large open circles) and the broken curve (small open circles) correspond to the curves of Fig. 8. An absolute calibration has been introduced, giving the number of galaxies per magnitude class in 1 Mpc³. The calibration is based on the space density, 0.17 galaxies brighter than $M = -15.0$ per Mpc³, that is derived in sect. 14–15. It should be pointed out here that the distribution curves may be assumed to represent an average volume of space, since the satellite population investigated presumably approaches a random sample of all general field galaxies (cf. sect. 1).

In Fig. 10 two interesting comparisons are made with results available from other sources. The open squares represent the three nearby galaxy groups listed in Table 1, a material that is probably complete down to $M = -13.5$. The class frequencies are, except in the faintest class (five galaxies), overlapping means, 50 % from the central class and 25 % from each adjoining class. In spite of the small total number, only 18, there is a good agreement with the full curve. It should be remarked that the Milky way and M81 have been omitted, as being the central systems in the Local Group and the M81 group. The large filled circles represent all the galaxies in the redshift lists to be analysed in sect. 15, whereas the small filled circles refer to the E–So–Ir galaxies alone. It is very satisfactory to find that the luminosity curves derived from the redshift material are in perfect agreement with the curves from the satellite groups, especially in view of the fact that in the brighter magnitude classes the former curves are based on a much larger number of objects.

To summarize the results obtained in this section, it can be stated that the total luminosity function (pg) referring to all galaxies in 1 Mpc³ (general field) is described by the expression:

$$\varphi(M) = 40 \cdot 10^{0.195M} + 0.025 \cdot e^{-0.35(M+17.7)^2}, \qquad (2)$$

where the first part refers to types E–So–Ir, and the second part to types Sa–Sb–Sc. The formula represents the distribution from $M = -10.6$ to $M = -19$ or -20; beyond this limit the curve rapidly approaches zero. Whereas the total number of galaxies is 0.17 per Mpc³ for magnitudes brighter than -15.0, it increases to about 0.8 for $M \leqslant -10.6$. It should be recollected that the luminosity function is based on a Hubble parameter of 80 km/sec per Mpc.

In conclusion, some results will be given that refer to different classes of morphological type. In the interval $M < -14.2$ there are 34 E–So objects, 19 Ir I objects, and 8 Ir II objects, as is clear from Table 5. For the interval $M < -15.0$, where Sa–Sb–Sc spirals are more fully represented, the relative frequencies range from 34 % (Sc) to

Table 5. Division of the material into separate type classes.

The table lists the number of physical companions in the 160 survey areas that have $M < -15.0$ ($M < -14.2$), and the mean absolute pg magnitude corresponding to a given class of apparent magnitude.

Type	Number		$\overline{M}_m$
E–So	(34)	23 = 30 %	−19.8
Ir I	(19)	13 17	−17.5
Ir II	(8)	5 7	(−19.0)
Sa–Sb		9 12	−20.0
Sc		26 34	−19.2

7 % (Ir II). These figures naturally refer to physical members of the 160 satellite groups (optical companions eliminated). The mean absolute magnitude corresponding to a given volume of space cannot be determined for E–So–Ir galaxies; for Sa–Sb–Sc spirals the mean magnitude is -17.7, as stated above. It is however possible to compute, by means of the luminosity functions, the mean absolute magnitude that would correspond to a given class of apparent magnitude. The results are listed in the last column of Table 5. The mean magnitudes are to some extent based on a combination of the present data and the Holmberg (1964) catalogue, which is complete as regards galaxies of bright apparent magnitudes.

13. Magnitude distribution in the Virgo cluster

In previous attempts to determine the luminosity function for galaxies the Virgo cluster has sometimes been included, the cluster being of a loose irregular type that possibly does not differ too much from the general field, as regards population. The distance of the cluster can be determined with a comparatively high degree of accuracy. According to the writer (1964), both redshifts and photometric data (Hubble parameter $=80$) indicate an absolute modulus of 30.5; in a recent analysis of data referring to globular clusters in M87, Sandage (1968) has found a slightly larger modulus. It would naturally be of interest to compare the luminosity function of the cluster members with the general field function derived in the preceding sections.

For the brighter cluster members photometric determinations of apparent pg magnitude are available, in the first place, in Holmberg (1958) and Humason *et al.* (1956). For the fainter members, down to $m=15.5$, magnitudes may be obtained from the comprehensive survey lists published by Zwicky and his collaborators (1961, 1963).

As a first step, the systematic errors in the Zwicky magnitude scale (Z) will be examined. Since the magnitudes have been estimated on small-scale Schraffier films, and since they have been reduced to the Shapley-Ames (1932) system, systematic deviations from the photometric lists must be expected. A plot of the magnitudes against the photometric determinations indicates that the systematic error is small at the limit $Z=15.5$, also for galaxies brighter than $Z=11.5$, but that in the intermediate interval the Z magnitudes are too faint by about half a magnitude. Since the systematic error presumably depends on the type and the surface magnitude of the object, and since the photometric lists in the faint magnitude classes are dominated by concentrated E and So galaxies, a more reliable result may be obtained if the statistical distribution of the uncorrected Zwicky magnitudes referring to all the galaxies in the general field (all the Zwicky survey fields outside the Virgo area) is compared with the corresponding distribution derived from photometric magnitudes. The latter may be represented by the distribution function (cf. sect. 14) that has been previously determined by the writer (1958) for general field galaxies. If the Z magnitudes are referred to the galactic pole by the Hubble (1934) absorption correction, a comparison between the two distribution curves leads to corrections to the Z magnitudes of -0.1 ($Z=15.5$), -0.3 ($Z=15.0$), -0.5 ($Z=14.5$), -0.6 ($Z=14.0-12.5$), and -0.4 ($Z=12.0$). Above the 12th magnitude, photometric results are available for practically all galaxies. It should be noted that at the fainter end of the Z scale the corrections given include a small redshift effect.

The resulting distribution of absolute pg magnitudes for Virgo cluster members, as based on the corrected Z magnitudes and all available photometric determinations,

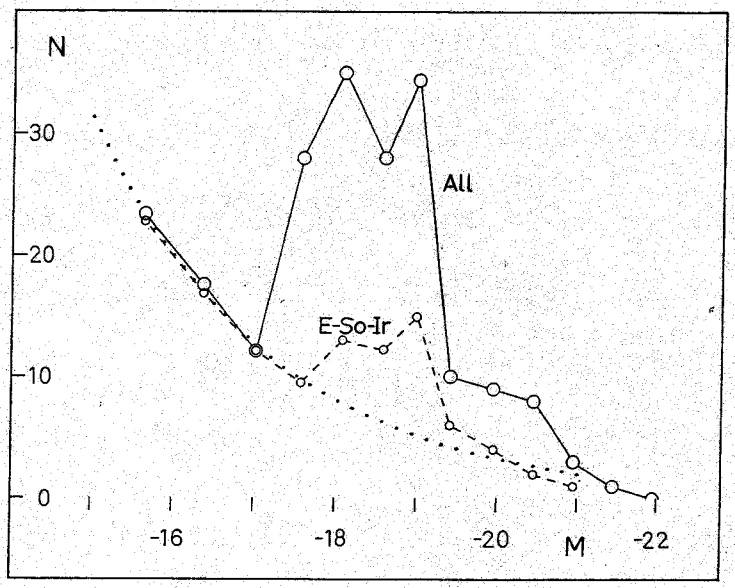

Fig. 11. Statistical distributions of absolute pg magnitudes of members of the Virgo cluster. For comparison, the broken curve of Fig. 10 has been reproduced as a dotted line.

is reproduced in Fig. 11. The background–foreground field has been subtracted, as is described below. The distribution refers to all physical members within an elliptical area extending in right ascension from 12^h08^m to 12^h48^m and in declination from $+2°.5$ to $+18°.5$ (1950; cf. Holmberg 1958) that are included in the Zwicky survey lists ($Z \leqslant 15.5$). The apparent pg distance modulus has been assumed to be 30.75. As before, the full curve refers to galaxies of all types, whereas the broken curve represents E–So–Ir galaxies alone; the morphological types have been estimated by the writer on the Sky Atlas prints. For comparison, the distribution curve for the E–So–Ir group in Fig. 10 has been introduced as a dotted line, adjusted to fit the cluster frequencies in the three faintest magnitude classes. It should be noted that the frequencies in the figure are all reduced to a class breadth of half a magnitude.

The disturbance from the background–foreground field is rather serious, especially in the fainter magnitude classes. The number of optical members in each class has been determined by means of the apparent magnitude distribution curve (general field) referred to above. The optical members have been divided into the groups E–So–Ir and Sa–Sb–Sc by means of the luminosity functions of Fig. 10, which are assumed to represent the background–foreground population; an analysis based on these curves shows that a selection by apparent magnitude would lead to a mixture of about 39 % E–So–Ir and 61 % Sa–Sb–Sc (constant space density).

The present investigation leads to a total number of physical cluster members of about 221 down to the limiting absolute magnitude -15.3, and a total number of optical members of about 338; the mean relative number of physical members is thus 40 %. In the last magnitude class, however, the relative frequency of physical members is reduced to 14 %. It may be recollected that in the satellite groups investigated this unfavorable ratio was reached first in the class centered on $M = -11.2$ (cf. Table 4); in a class centered on $M = -15.5$ it would be about 75 %. These figures reflect the large difference in space density. Whereas the satellite groups have an average density of galaxies brighter than $M = -15.0$ of about 100 per Mpc^3 (cf. sect. 14), the corresponding density in the Virgo cluster, as defined here, is estimated at about 20.

The results presented in Fig. 11 show that the luminosity function for cluster members of types E–So–Ir agrees rather well with the function found for the satellite groups. The only deviation is a certain excess of cluster members in the interval $M = -18$ to -19.5. This hump may perhaps correspond to the secondary maximum found by Abell (1962) in the luminosity functions of several clusters; it may be noted that Abell's results refer to dense clusters, where the Sa–Sb–Sc group is practically non-existent. In the case of spiral galaxies there are interesting differences between Fig. 11 and Fig. 10. Whereas the absolute magnitudes of Sa–Sb–Sc systems in the general field extend to about $M = -15$, there seems to be a rather well-defined limit in the Virgo cluster close to $M = -17$; beyond this magnitude there are no spiral systems at all. On the other hand, the relative number of spiral galaxies of high luminosity is about twice as high as in the general field.

Chapter V. Space density and mass function

14. Space density from magnitudes and diameters

In the calibration of the luminosity function of Fig. 10 the smoothed-out space density of galaxies brighter than $M = -15.0$ (outside the big clusters) has been assumed to be 0.17 per Mpc^3. This figure represents a mean result derived from the analyses in this and the next section of the magnitudes, diameters, and redshifts of galaxies.

For comparison, it may be noted that the average space density in the 160 satellite groups investigated amounts to about 100 per Mpc^3. The volume corresponding to each group is represented by a cylinder, pointing towards the observer, with a radius of 50 kpc and a length of about 600 kpc; the total volume corresponding to all the groups is equal to 0.75 Mpc^3. The total number of satellites brighter than $M = -15.0$ is 74 (down to the limit $M = -10.6$ the total number is about 370).

In order to derive the space density from the magnitudes, it is necessary to have access to (*a*) the statistical distribution of the apparent magnitudes for a representative sample of galaxies, and (*b*) the distribution of the absolute magnitudes. As regards the former distribution, the curve previously derived by the writer (1958) may be used. The curve refers to all Shapley-Ames (1932) galaxies over the entire sky, with the exception of the galactic belt (gal. lat. $-30°$ to $+30°$) and the Virgo cluster area. The Sh–A magnitudes have been individually reduced to the writer's photometric pg system by corrections that are mainly a function of the surface magnitudes of the objects; the mean error of the corrected magnitudes amounts to 0.3 magn. If the magnitudes are freed from the entire amount of galactic absorption by means of the Hubble (1934) cosecant-law, the statistical distribution is described by

$$\log N(m) = 0.6m - 8.72, \qquad (3a)$$

where $N(m)$ is the total number of galaxies brighter than m in one square degree of of the sky. The inclination of the distribution line indicates a space density of galaxies that is independent of the distance.

The distribution function agrees comparatively well with the results obtained by Hubble (1934) from counts of galaxies on Mount Wilson plates. If Hubble's limiting magnitudes are corrected for redshift effect, and for systematic errors in the stellar magnitudes in the Selected Areas that were used for comparison, the constant term in the log. distribution will be approximately the same as that given in eq. (3*a*). It

may be pointed out in this connection that an evaluation of the *effective* limiting magnitude is a rather complicated problem, since the limit is no doubt a function of the galaxian type. A comparison with the distribution of galaxies, as derived by Shane and Wirtanen (1967) from the Lick Observatory counts of galaxies, has to await a definitive determination of the effective limiting magnitude.

According to well-known relations in stellar statistics, the space density $D(1\,\mathrm{Mpc}^3)$ of galaxies brighter than the absolute magnitude M' is obtained from the equation

$$N(m) = 1.02\, D \cdot 10^{-19+0.6m} \cdot \int_{-\infty}^{M'} \varphi(M) \cdot 10^{-0.6M} dM, \qquad (3\,b)$$

assuming that the density, and the luminosity function $\varphi(M)$, are independent of the distance. The integral can be determined by a numerical integration based on the curve of Fig. 10; it should be noted that in this case $\varphi(M)$ is the *relative* distribution function. If the limiting magnitude M' is made equal to -15.0, the integral has a value of $1.19 \cdot 10^{11}$.

If eqs. (3 *a*) and (3 *b*) are combined, it is found that $D = 0.16$. Since the result is based on a Hubble parameter $H = 80$ km/sec per Mpc, it can be written in the following way:

$$D = 0.16\ (H/80)^3 \text{ per Mpc}^3, \qquad (3\,c)$$

in order to correspond to any assumed value of H. The result refers to a limiting pg magnitude $M' = -15.0$ but can easily be reduced to other values of M' by means of the luminosity curve of Fig.10 (and Fig. 8).

The statistical distribution of the apparent diameters of galaxies needed for the determination of space density from diameters can be derived from the present material. Measures of major diameters are available for over 3000 galaxies in the survey areas and comparison areas. The homogeneity of this material has been discussed in sect. 5; except for a certain decrease in the number of very small galaxies, presumably a redshift effect, the distribution of the diameters appears to be consistent with the assumption of a space density independent of the distance. If the smallest diameters are left out, the distribution of the log. diameters (as reduced to the writer's photometric diameter system; cf. sect. 10) of the galaxies in all the survey areas and comparison areas is described by the relation

$$\log N(\log a) = -3 \log a + 0.43, \qquad (4\,a)$$

where $N(\log a)$ is the total number of galaxies in one square degree having diameters larger than a (min. of arc). The space density is in this case obtained from the equation

$$N(\log a) = 4.1 D \cdot 10^{-12-3 \log a} \cdot \int_{\log A'}^{+\infty} \varphi(\log A) \cdot 10^{3 \log A}\, d \log A, \qquad (4\,b)$$

where $\varphi(\log A)$ is the relative distribution of the log. absolute major diameters (pc), which is assumed to be independent of the distance. The space density refers to all galaxies having absolute diameters larger than the limit A'. If the latter diameter is made equal to 5000 pc, corresponding approximately to an absolute magnitude of -15.0 (cf. eq.1), a numerical integration based on the curve of Fig. 8 gives a value for the integral of $4.5 \cdot 10^{12}$. Accordingly, the space density is equal to 0.15 per Mpc^3.

Although it is difficult to define exactly the absolute diameter that would correspond to the above limiting magnitude $M' = -15.0$, it is satisfactory to note that the space density found from the diameters is nearly the same as the density derived from the magnitudes.

15. *Space density from redshifts*

The determination of space density is based on the redshifts listed in the Reference Catalogue by de Vaucouleurs *et al.* (1964), including a later addition by the same authors (1967). In order to have a material as homogeneous as possible, only the northern galactic hemisphere above $B^{II} = +30°$ has been included; below this latitude it is difficult to estimate the degree of completeness of the material, as well as the systematic selection effects. To avoid all disturbances from the Virgo cluster, a rather large region ($\alpha = 12^h - 13^h$, $\delta = -10° - +20°$) has been excluded; the remaining area amounts to 23.9 % of the entire sky. The apparent pg magnitudes have, in order of preference, been taken from Holmberg (1958), Humason *et al.* (1956), and (in a few cases) the Reference Catalogue. All magnitudes have been corrected for galactic absorption by $-^m25$ csc B^{II}; since the maximum redshift (corr. for solar motion) is 4000 km/sec, the magnitudes are free from any appreciable redshift effects.

Table 6 presents the distributions of the corrected magnitudes and logarithmic redshifts for all the galaxies (in the redshift lists) located in the above area. Each square of the table gives the number of objects, as well as the mean absolute pg magnitude corresponding to a Hubble parameter $H = 80$; the absolute magnitude ranges from -16.5 to -21.5. The table makes possible a check of the marginal distributions of apparent magnitude and redshift. As regards the magnitude, it seems quite clear that the interval $m = 11 - 12$ is under-represented. For $m < 11$ the magnitude distribution can be described by a logarithmic expression of the same type as that of eq. (3 *a*); if the distribution is reduced to one square degree, the constant term will be about the same

Table 6. Magnitude-redshift table for galaxies of all types with known redshifts ($B^{II} > +30°$; Virgo cluster area not incl.).

The columns represent different intervals of apparent pg magnitude (corr. for gal. abs.), and the rows intervals of log. redshift (km/sec as red. to the gal. center). The absolute magnitudes ($H = 80$) corresponding to the different squares are given in brackets.

log. redshift	8^m–9^m	9^m–10^m	10^m–11^m	11^m–12^m
2.4–2.6	3 (−19.5)	3 (−18.5)	5 (−17.5)	1→2 (−16.5)
2.6–2.8	2 (−20.5)	7 (−19.5)	6 (−18.5)	7→15 (−17.5)
2.8–3.0	1 (−21.5)	5 (−20.5)	21 (−19.5)	23→49 (−18.5)
3.0–3.2	—	1 (−21.5)	27 (−20.5)	36→77 (−19.5)
3.2–3.4	—	—	2 (−21.5)	38→82 (−20.5)
3.4–3.6	—	—	—	10→22 (−21.5)

or -8.68, which indicates that the redshift material is essentially complete down to $m=11$. In order to agree with this distribution, the frequencies of the interval $m=11-12$ have to be multiplied by the factor 2.15; the corrected frequencies are also listed in the table. It may be pointed out here that it would be impossible to pursue the investigation to fainter magnitudes; in the interval $m=12-13$ the correction factor is increased to about 10.

In a renewed analysis, the procedure is repeated for galaxies belonging to the type group E–So–Ir, their total number down to $m=12$ being 65; with the same correction factor in the interval $m=11-12$ the number is increased to 114. The morphological types have been taken from the original redshift lists, attention being paid to the information given in the Reference Catalogue.

Summations along the diagonals of the distribution tables give the total numbers referring to the different classes of absolute magnitude; divisions by the corresponding volumes lead to the space densities. As appears from Table 6, reliable results can be obtained only for absolute luminosities higher than $M=-17.0$. The densities, as referred to 1 Mpc^3, have been plotted in Fig. 10. The results are in perfect agreement with the luminosity curves derived from the satellite groups.

It should be noted that the results have not been corrected for possible disturbances by the peculiar motions of the galaxies. A detailed analysis of the redshift distributions corresponding to the different classes of apparent magnitude shows that the theoretical corrections would be small, and that they would partly be of opposite sign, as compared to the corrections indicated for the luminosity curve derived from the satellite groups. Since the fluctuations in the individual class frequencies of the magnitude–redshift tables are considerable, and since there may remain systematic selection effects in the material (especially in the class $m=11-12$), it did not seem possible to derive any corrections that would be statistically significant.

By means of an extrapolation based on the luminosity curve of Fig.10, the above analysis leads to a total space density of galaxies brighter than $M=-15.0$ of 0.18 per Mpc^3. The integrated result is practically independent of any disturbance that may be caused by the peculiar motions of the galaxies. The result is in good agreement with those obtained from the magnitudes and the diameters.

The total space density derived here agrees with the result obtained by Kiang (1961) in a similar analysis of galaxian redshifts. On the other hand, the luminosity functions do not agree, due to the fact that Kiang's curve is based on the assumption that the redshift material represents a selection according to the apparent magnitude, and to the fact that in the fainter magnitude classes the material has been increased by the incorporation of data of questionable quality. In the writer's opinion, the redshift material available for the present does not permit the drawing of any reliable conclusions about the luminosity function below $M=-17$.

16. The mass function

The results available so far may be used as a basis for the determination of the smoothed-out space densities of luminosity and mass, and of the statistical distribution of the masses of galaxies (general field).

The pg luminosity density or the total amount of luminosity in 1 Mpc^3 is obtained by a numerical integration based on the curves of Fig. 10 and Fig. 8; the most luminous galaxies make the largest contribution. The result is $1.8\cdot10^8$ solar units for the

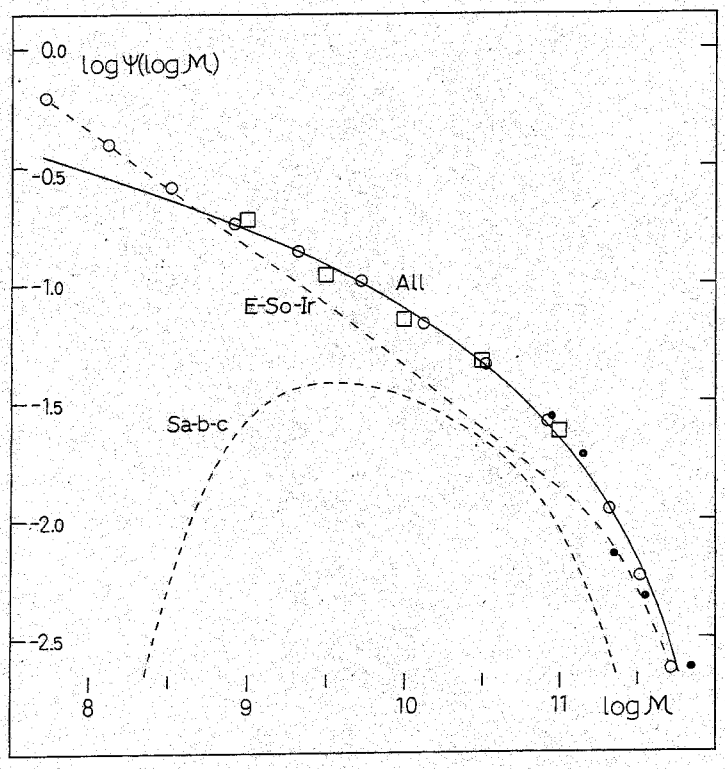

Fig. 12. Statistical distribution (1 Mpc^3) of the log. masses (solar units) of the 274 satellites. The circles give the sum of the distributions corresponding to types E–So–Ir and Sa–Sb–Sc (broken curves). The squares refer to the Local Group and M81 group, and the filled circles to nearby galaxies in the Holmberg (1964) catalogue. The full curve represents the adopted analytical mass function (eq. 5).

E–So–Ir type group, and $2.3 \cdot 10^8$ solar units for the Sa–Sb–Sc group. The absolute pg magnitude of the sun has been assumed to be $+5.37$.

The mass density may be derived from the luminosity density, if the mean mass-luminosity ratio can be estimated. The results obtained in a previous study by the writer (1964) indicate the following ratios: 22 (E–So), 12 (Sa–Sb), 2.7 (Sc), and 1.2 (Ir I), both masses and luminosities being measured in solar units (for the few Ir II systems a ratio of 10 may be adopted). With the relative frequencies listed in Table 5, the mean ratios for the E–So–Ir and Sa–Sb–Sc groups would be 14 and 5, respectively. Accordingly, the mass density for the first group is $25 \cdot 10^8$, and for the second $12 \cdot 10^8$ solar units. The total density is $37 \cdot 10^8$ solar masses per Mpc^3, or $2.5 \cdot 10^{-31}$ gr/cm^3. It should be noted that the density is based on a Hubble parameter $H = 80$, that it refers to the general field (the mass contributed by the big clusters would however be comparatively small), and that it does not include gas or other dark matter in the intragalactic space. It may be added that in a recent discussion, based on earlier analyses of the observation data available, Peebles and Partridge (1967) have arrived at a mean mass density that is in good agreement with the result found here.

In order to determine the statistical distribution of the masses of all galaxies in a given volume of space, or the mass function, it is necessary to have more detailed information on the luminosity functions corresponding to the separate morphological types. Galaxies of types E–So, Ir I, and Ir II will all be assumed to have the same luminosity function, the curve of Fig. 10 (Fig. 8), with the limitations that the maximum luminosity for Ir I is assumed to be $M = -19.5$, and for Ir II -20.5, whereas the E–So objects proceed to the upper limit of -22.0; these cut-offs are indicated

from studies of the Holmberg (1964) material and the redshift lists. It was found in sect. 12 that the mean magnitude for the Sa–Sb–Sc group is $M = -17.7$. A detailed study of the present material, combined with the lists mentioned, seems to justify an attempt to subdivide this group. The mean absolute magnitudes are found to be approximately -18.0 (Sa), -18.4 (Sb), -18.0 (Sc$-$), and -17.1 (Sc$+$); with relative frequencies of 6 %, 20 %, 28 %, and 46 %, respectively, the weighted mean of the magnitudes will be -17.7. The large increase in relative number from Sa to Sc$+$ may seem surprising but is indicated by the material at hand. The luminosity function for each spiral type will be assumed to be a normal error-curve, centered on the mean magnitude and with a dispersion of 1.1 magn.; the combined dispersion for all the types will then amount to 1.2 magn., as was found in sect. 12. It should be remarked that the luminosity curve suggested for each of the six type classes is necessarily of an approximate nature, but that the individual deviations may tend to be smoothed out when all the curves are combined.

With rounded-off mass-luminosity ratios of 22 (E–So), 17 (Sa), 10 (Ir II), 9 (Sb), 3 (Sc–), 2 (Sc$+$), and 1.2 (Ir I), the luminosity curves are transformed into the combined mass distributions for the E–So–Ir and Sa–Sb–Sc groups that are reproduced in Fig. 12 (broken curves). The scale on the ordinate axis gives an absolute calibration, or the logarithmic number per unit of log. mass per Mpc^3. The two curves have been adjusted to fit this calibration, that is, the total mass corresponding to each curve agrees with the mass density derived above for the E–So–Ir group and the Sa–Sb–Sc group. The open circles represent the final mass function or the sum of the two curves.

It is found that the final mass function, represented by the full curve in the figure, can be described by a simple analytical expression:

$$\psi(\log \mathcal{M}) = 0.018(12.1 - \log \mathcal{M})^2, \tag{5}$$

which gives the number of galaxies per Mpc^3 having masses referring to a unit interval of $\log \mathcal{M}$. The numerical parameters have been determined by a least-squares solution, based on the class frequencies in the interval of log. mass from 8.9 to 11.3. The individual frequencies (open circles) show a very good agreement with this curve. The only deviations are found for log. masses below 8.5; even for this interval the curve may possibly approximate to the true mass distribution, since the mass-luminosity ratios for these dwarf galaxies have probably been over-estimated. It may be noted that the parameter within the brackets of eq. (5) has a special significance, since it apparently represents the log. maximum mass of galaxies.

In Fig. 12 comparisons have been made with data available from other sources. The squares refer to the Local Group and the M81 group, listed in Table 1. Although the total number of galaxies is small, the successive class frequencies (overlapping means) agree well with the adopted curve. The filled circles represent the most massive galaxies in the Holmberg (1964) list, which is apparently complete, as regards galaxies with log. masses larger than 10.8 (total number = 54). Even in this case, there is a good agreement with the full curve.

The mass function can be presented in a different way, which may be of interest from a cosmological point of view. The curve of Fig. 13 represents the function $\mathcal{M} \cdot \varphi(\mathcal{M})$ or the total mass of all galaxies in 1 Mpc^3 that have masses referring to a unit interval of $\mathcal{M}$. If all galaxies were formed directly from the primeval gas, as is usually postulated, the curve would describe an important feature of the original con-

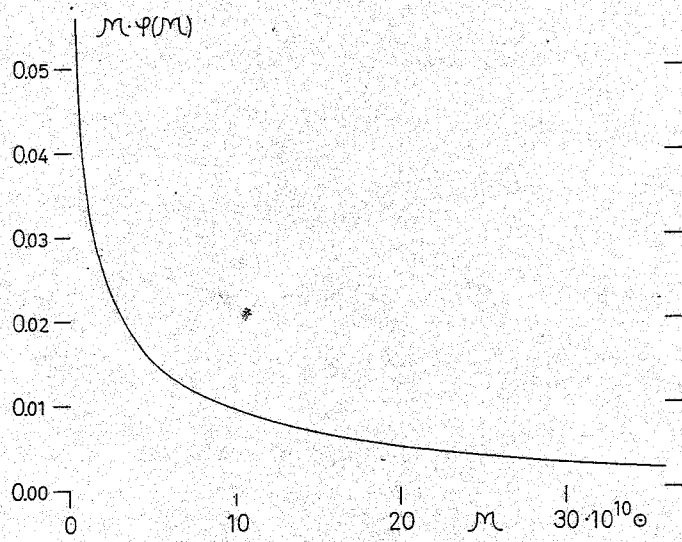

Fig. 13. The mass function presented in a different way. The curve gives the total mass of all galaxies in 1 Mpc^3 that have masses referring to a unit interval of mass.

densation process, that is, it would show the total amount of gas that went into the formation of galaxies of different mass. As is easily proved, the statistical distribution of galaxian masses, $\varphi(\mathcal{M})$, is equal to the function $\psi(\log \mathcal{M})$, multiplied by the factor $\log e/\mathcal{M}$; accordingly, the function $\mathcal{M}\cdot\varphi(\mathcal{M})$ will be equal to $0.0078\ (12.1-\log \mathcal{M})^2$. An integration of this function leads to $37\cdot10^8$ solar units, or the mass density that was derived above. We find that galaxies with log. masses above 11.0 contribute about 46 o/o of the total mass in a given volume of space, and that galaxies with log. masses in the intervals 10–11 and 9–10 represent 40 o/o and 11 o/o, respectively. The contribution by galaxies with masses below 10^9 solar units is so small, less than 3 o/o, that it may be neglected. These figures refer to the general field, but an inclusion of the big clusters of galaxies would presumably not change the results to any great extent.

In conclusion, it may be added that there is an unexpected agreement between the mass function for galaxies and the mass function for stars. It seems possible to describe the initial stellar-mass function, as derived by Limber (1960), by an analytical expression of the same type as that given in eq. (5). A least-squares solution, based on the frequencies of log. stellar masses in the interval 0.0 to +2.0, gives a distribution = const. $(2.5-\log \mathcal{M})^2$. The numerical parameter within the brackets may also in this case represent the maximum log. mass of the initial gas cloud (although condensations of this size do not give birth to stable stars). It is an interesting question whether this agreement is a coincidence or whether it may be interpreted as indicating that the condensation processes leading to the formation of galaxies and of stars both follow the same general law.

Table 7. Observational data.

The table lists all the 174 spiral systems that have been included in the survey work. The successive columns give the NGC number, the class to which the galaxy has been referred (cf. sect. 4), the morphological type in the revised Hubble system, the nuclear color excess (cf. sect. 6), the adopted absolute distance modulus, the observed number of companions within 50 kpc (diam. $\geqslant 1.0$ kpc), and the accepted number of physical companions.

NGC	Class	Type	ΔC_N	$m-M$	N_{obs}	N_{phys}
24	A	Sc –	—	29.5	4	+1
224	A	Sb –	+0.07	24.18	2	+2
247	A	Sc +	—	28.0	6	+4
253	A	Sc	—	28.0	1	0
598	B	Sc +	+0.13	24.18	0	0
628	B	Sc –	+0.01	29.7	8	+5
672	C	Sc +	−0.09	28.7	7	+5
784	A	Sc +	—	28.7	2	+1
891	A	Sb +	—	29.4	6	+4
908	A	Sc –	+0.14	30.8	2	0
925	B	Sc +	−0.11	29.4	2	−1
936	B	So	+0.04	30.8	12	—
1003	A	Sc +	−0.09	29.4	13	—
1023	A	So	0.00	29.4	5	+3
1042	C	Sc –	+0.06	30.2	8	+5
1055	C	Sb +	+0.01	28.0	6	+5
1058	B	Sc –	−0.12	29.4	10	—
1090	C	Sb +	−0.15	28.9	7	+5
1232	B	Sc –	+0.18	30.7	2	−1
1300	B	Sb +	−0.01	30.9	3	0
1325	C	Sb +	−0.07	31.0	5	+2
1337	A	Sc +	+0.21	29.3	1	−2
1507	A	Sc	—	30.1	2	−1
1560	A	Sc +	—	28.0	2	0
1637	B	Sc –	+0.14	29.5	3	0
1784	B	Sc –	+0.19	29.8	4	+1
2146	B	Sc –	—	30.1	7	+4
2403	A	Sc +	−0.04	27.60	6	+5
2541	A	Sc +	−0.04	29.0	1	0
2613	A	Sb	—	31.2	6	+2
2681	B	Sa	−0.17	30.9	5	+2
2683	A	Sb –	−0.07	29.8	2	0
2685	B	So	0.00	30.4	5	+2
2715	A	Sc –	−0.04	30.8	4	+2
2835	B	Sc –	—	29.5	1	−2
2841	A	Sb –	−0.03	30.1	9	—
2903	B	Sc –	−0.03	29.5	3	0
3003	A	Sc	—	30.2	2	0
3027	C	Sc +	—	30.1	5	+2
3031	C	Sb –	0.00	27.30	8	+7
3044	A	Sc	—	30.8	6	+3
3079	A	Sc –	—	30.2	3	0
3166	C	Sa	−0.06	31.0	6	+3
3184	B	Sc –	+0.08	29.3	1	−2
3190	C	Sa	−0.04	30.8	7	+4

Table 7 (*cont.*)

NGC	Class	Type	ΔC_N	$m-M$	N_{obs}	N_{phys}
3198	A	Sc –	+0.14	29.1	2	+1
3227	C	Sb	—	30.5	7	+4
3239	B	Sc +	—	29.9	10	—
3254	A	Sb +	—	30.8	1	−1
3301	A	So	—	31.0	4	+1
3310	B	Sb +	—	30.7	2	−1
3319	A	Sc +	−0.05	29.3	3	0
3338	B	Sc –	+0.24	29.8	7	+4
3344	B	Sc –	+0.03	29.6	6	+3
3351	B	Sb +	0.00	29.8	1	−2
3359	B	Sc +	−0.11	30.2	7	+4
3368	B	Sa	+0.02	29.8	1	−2
3384	C	So	—	29.7	6	+3
3423	B	Sc +	+0.14	29.8	5	+2
3432	A	Sc +	−0.12	29.8	5	−1
3447	B	Sc +	—	30.1	7	+4
3486	B	Sc –	+0.09	29.6	4	+1
3495	A	Sc	—	30.1	6	+2
3510	A	Sc	—	29.6	5	+3
3511	C	Sc	—	30.4	2	−1
3521	A	Sb –	+0.01	29.2	8	+5
3556	A	Sc +	—	29.6	7	+2
3623	C	Sa	−0.06	29.8	2	−1
3627	C	Sb +	−0.02	29.8	2	−1
3628	C	Sb +	—	29.8	5	+2
3631	B	Sc –	−0.23	30.6	3	0
3642	B	Sc –	−0.10	30.3	7	+4
3675	A	Sb –	—	29.8	1	−1
3726	B	Sc –	−0.11	30.3	6	+3
3756	C	Sc –	0.00	30.4	6	+3
3810	B	Sc –	+0.10	29.8	12	—
3893	B	Sc –	—	30.6	5	+2
3898	B	Sa	—	30.8	7	+4
3938	B	Sc –	+0.07	30.8	7	+4
3953	B	Sb +	−0.01	30.2	8	+5
3992	B	Sb +	+0.18	30.2	9	—
4026	A	So	—	30.4	3	0
4051	B	Sb +	−0.11	30.1	2	−1
4064	A	Sa	—	30.4	5	+2
4088	A	Sc –	0.00	31.0	6	+4
4096	A	Sc +	+0.13	30.3	1	−1
4111	C	So	−0.07	30.2	11	—
4116	C	Sc +	+0.03	30.5	3	0
4123	C	Sc –	+0.03	30.5	3	0
4151	B	Sa	—	30.5	8	+5
4178	A	Sc +	+0.11	30.5	2	0
4192	A	Sb +	+0.05	30.2	6	+3
4206	C	Sc –	—	29.7	11	—
4216	A	Sb –	+0.11	29.7	11	—
4235	C	Sa	+0.06	30.5	8	+5

Table 7 (*cont.*)

NGC	Class	Type	ΔC_N	$m-M$	N_{obs}	N_{phys}
4236	A	Sc +	—	25.9	5	+3
4242	B	Sc +	0.00	29.5	2	−1
4244	C	Sc +	—	27.1	0	−1
4254	B	Sc −	+0.07	30.5	1	−2
4258	A	Sb +	−0.09	29.0	7	+4
4274	C	Sa	+0.09	30.0	7	+4
4293	A	Sa	—	29.7	2	0
4298	C	Sc −	+0.06	30.5	4	+1
4302	C	S	—	30.5	6	+3
4303	C	Sc −	+0.06	30.5	5	+2
4314	B	Sa	—	30.2	5	+2
4321	B	Sc −	−0.13	30.5	7	+4
4371	B	So	+0.01	30.5	9	—
4374	C	So	+0.02	30.5	8	+5
4382	C	So	−0.01	30.5	3	0
4395	B	Sc +	0.00	27.1	0	−1
4414	B	Sc −	—	29.8	13	—
4429	B	So	+0.07	30.5	2	−1
4442	C	So	−0.02	30.5	11	—
4448	A	Sb −	—	29.7	9	—
4450	B	Sb −	+0.04	30.5	4	+1
4490	C	Sc +	−0.09	30.5	2	−1
4496	C	Sc +	—	30.5	4	+1
4501	B	Sb +	+0.12	30.5	2	−1
4517	A	Sc −	—	29.7	4	+2
4527	A	Sb −	+0.13	30.5	2	−1
4535	B	Sc −	+0.02	30.5	6	+3
4536	A	Sc −	+0.10	30.5	5	+3
4548	B	Sb +	−0.03	30.5	3	0
4559	B	Sc +	+0.19	29.7	3	0
4565	A	Sb +	—	29.4	6	+2
4567	C	Sc −	—	30.5	8	+5
4568	C	Sc −	—	30.5	8	+5
4569	A	Sb +	−0.17	30.5	5	+1
4571	B	Sc +	+0.23	30.5	2	−1
4579	B	Sb −	−0.02	30.5	3	0
4586	C	Sa	+0.22	30.5	4	+1
4594	A	Sa	+0.11	30.5	3	−1
4596	C	Sa	+0.10	30.5	3	0
4618	C	Sc +	−0.15	30.4	5	+2
4631	C	Sc +	—	28.6	7	+5
4651	B	Sc −	−0.02	30.5	4	+1
4654	C	Sc −	+0.11	30.5	5	+2
4665	B	So	—	30.5	1	−2
4666	A	Sc −	+0.01	30.5	5	+3
4689	B	Sc −	+0.03	30.5	3	0
4698	B	Sa	−0.01	30.5	2	−1
4710	A	So	—	30.6	1	−1
4725	B	Sb +	−0.03	30.2	5	+2
4736	B	Sb −	—	29.4	2	−1

Table 7 (*cont.*)

NGC	Class	Type	ΔC_N	$m-M$	N_{obs}	N_{phys}
4754	C	So	—	30.8	2	−1
4762	C	So	—	30.8	2	−1
4781	C	Sc+	—	29.9	4	+1
4826	B	Sb−	+0.07	29.9	1	−2
4856	A	Sa	—	30.5	7	+3
4941	B	Sb−	—	30.5	4	+1
5033	C	Sc−	+0.02	29.3	3	0
5055	B	Sb+	−0.11	29.3	5	+2
5194	C	Sc−	—	29.8	3	0
5204	A	Sc+	−0.11	29.1	5	+2
5364	C	Sc−	+0.24	30.0	3	0
5457	C	Sc−	0.00	27.7	7	+6
5474	C	Sc+	−0.04	29.1	1	−1
5585	B	Sc+	−0.04	29.1	0	−2
5746	A	Sb−	+0.11	31.2	5	+2
5775	C	Sb+	—	31.0	8	+5
5866	A	So	—	30.4	5	+1
5879	A	Sb+	—	30.6	2	−1
5907	A	Sb+	—	29.0	4	+1
6015	A	Sc+	+0.20	30.6	0	−2
6503	A	Sc−	−0.14	29.6	3	+1
7331	A	Sb+	−0.09	30.2	7	+4
7361	A	Sc	—	30.9	1	−1
7640	A	Sc+	—	29.2	0	−1
7741	B	Sc+	−0.08	30.2	6	+3
7814	A	Sa	—	31.0	6	+3
239*	B	Sc−	−0.13	30.3	3	0
A 103	B	Sc+	—	30.6	6	+3
Rh 80	C	Sc+	—	29.7	3	0

REFERENCES

ABELL, G. O., Problems of Extra-Galactic Research, I. A. U. Symposium 15 (ed. G. C. McVittie), p. 213. Macmillan, New York (1962).
—— Ap. J. *140*, 1624 (1964).
ABELL, G. O., and EASTMOND, S., A. J. *73*, S 161 (1968).
ARP, H., Ap. J. *148*, 321 (1967).
—— P.A.S.P. *80*, 129 (1968 *a*).
—— Astrophyzika *4*, 59 (1968 *b*).
VAN DEN BERGH, S., A. J. *71*, 922 (1966).
—— J. R. astr. Soc. Can. *62*, 145, 219 = Commun. David Dunlap Obs., No. 195 (1968).
BURBIDGE, E. M., and BURBIDGE, G. R., Ap. J. *142*, 1351 (1965).
HOLMBERG, E., Ap. J. *92*, 200 = Contr. Mt Wilson Obs., No. 633 (1940).
—— Medd. Lunds astr. Obs., Ser. II, No. 128 (1950).
—— Medd. Lunds astr. Obs., Ser. II, No. 136 (1958).
—— Ark. Astr. *3*, 387 = Uppsala astr. Obs. Medd., No. 148 (1964).
HUBBLE, E., Ap. J. *79*, 8 = Contr. Mt Wilson Obs., No. 485 (1934).
—— Ap. J. *84*, 158 = Contr. Mt Wilson Obs., No. 548 (1936).
HUMASON, M. L., MAYALL, N. U., and SANDAGE, A. R., A. J. *61*, 97 (1956).
KIANG, T., M.N.R.A.S. *122*, 263 (1961).
LIMBER, D. N., Ap. J. *131*, 168 (1960).
LYNDS, C. R., and SANDAGE, A. R., Ap. J. *137*, 1005 (1963).

MINKOWSKI, R. L., and ABELL, G. O., The National Geographic Society – Palomar Observatory Sky Survey *in* Basic Astronomical Data (ed. K. Aa. Strand), p. 481. Univ. Chicago Press, Chicago (1963).
PEEBLES, P. J. E., and PARTRIDGE, R. B., Ap. J. *148*, 713 (1967).
REINMUTH, K., Veröff. Sternw. Heidelberg, Bd. 9 (1926).
SANDAGE, A., Ap. J. *152*, L 149 (1968).
SÉRSIC, J. L., and PASTORIZA, M., P.A.S.P. *79*, 152 (1967).
SÉRSIC, J. L., Bull. astr. Inst. Csl. *19*, 105 (1968).
SHANE, C. D., and WIRTANEN, C. A., Publ. Lick Obs., Vol. XXII, Part I (1967).
SHAPLEY, H., and AMES, A., Ann. Harv. Coll. Obs. *88*, 43 (1932).
SOLINGER, A. B., Ap. J. *155*, 403 (1969).
SWJAGINA, E. W., A. J. UdSSR *43*, 34 (1966).
DE VAUCOULEURS, G., and DE VAUCOULEURS, A., Reference Catalogue of Bright Galaxies, Univ. Texas Press, Austin = Univ. Texas Monogr. Astr., No. 1 (1964).
DE VAUCOULEURS, A., and DE VAUCOULEURS, G., A. J. *72*, 730 (1967).
WALKER, M. F., Ap. J. *151*, 71 (1968 *a*).
—— Astrophys. Letters *2*, 65 (1968 *b*).
ZONN, W., Acta astr. *18*, 335 (1968).
ZWICKY, F., Morphological Astronomy, Springer-Verlag, Berlin, p. 171 (1957).
—— Ap. J. *140*, 1626 (1964).
ZWICKY, F., HERZOG, E., and WILD, P., Catalogue of Galaxies and of Clusters of Galaxies, Vol. I. Cal. Inst. Techn., Pasadena (1961).
ZWICKY, F., and HERZOG, E., Catalogue etc., Vol. II, Cal. Inst. Techn., Pasadena (1963).
ZWICKY, F., KARPOWICZ, M., and KOWAL, C. T., Catalogue etc., Vol. V, Cal. Inst. Techn., Pasadena (1965).
ZWICKY, F., and HERZOG, E., Catalogue etc., Vol. III, Cal. Inst. Techn., Pasadena (1966).
ZWICKY, F., and HERZOG, E., Catalogue etc., Vol. IV, Cal. Inst. Techn., Pasadena (1968).
ZWICKY, F., and KOWAL, C. T., Catalogue etc., Vol. VI, Cal. Inst. Techn., Pasadena (1968).

Tryckt den 2 december 1969

Uppsala 1969. Almqvist & Wiksells Boktryckeri AB